CONTROLLED RELEASE of TEMOZOLOMIDE WITH HYDROXYPROPYL METHYL CELLULOSE (HPMC)-MODIFIED MONTMORILLONITE

MASTER'S THESIS

Firoozeh PANAHIANLARKEY

Advisor

Assoc. Prof. Dr. Hakan ÇİFTÇİ

NANOSCIENCE AND NANOTECHNOLOGY

February 2024

This thesis study was supported by Afyon Kocatepe University Scientific Research Projects Coordination Office with the project number 23.FEN.BİL.04

AFYON KOCATEPE UNIVERSITY
GRADUATE SCHOOL of NATURAL and APPLIED SCIENCES

MASTER'S THESIS

CONTROLLED RELEASE OF TEMOZOLOMIDE WITH HYDROXYPROPYL METHYL CELLULOSE (HPMC)-MODIFIED MONTMORILLONITE

Firoozeh PANAHIANLARKEY

Advisor
Assoc. Prof. Dr. Hakan ÇİFTÇİ

NANOSCIENCE AND NANOTECHNOLOGY

February 2024

SCIENTIFIC ETHICS NOTIFICATION PAGE

Afyon Kocatepe University

In this thesis study, which I prepared in accordance with the thesis writing rules of the Institute of Science and Technology;

- I have obtained all the information and documents in the thesis within the framework of academic rules,
- I present all visual, audio and written information and results in accordance with scientific ethical rules,
- In case of benefiting from the works of others, I cite the relevant works in accordance with scientific norms,
- I cite all the works I have cited as sources,
- I have not made any distortions in the data used,
- And I have not submitted any part of this thesis as another thesis work at this university or any other university.

I declare.

05/03/2024

Firoozeh PANAHIANLARKEY

ABSTRACT

MASTER'S THESIS

CONTROLLED RELEASE OF TEMOZOLOMIDE WITH HYDROXYPROPYL METHYL CELLULOSE (HPMC)-MODIFIED MONTMORILLONITE

Firoozeh PANAHIAN LARKEY

Afyon Kocatepe University

Graduate School of Natural and Applied Sciences

Department of Nanoscience and Nanotechnology

Advisor: Assoc. Prof. Dr. Hakan ÇİFTÇİ

This study examines the potential applications of montmorillonite (Mt) clay, both in its natural and as a suitable candidate for controlled drug release when modified with hydroxypropyl methylcellulose (HPMC). The main focus of the research specifically revolves around temozolomide (TMZ), which is a critical element for the treatment of glioblastoma. Inorganic composite such as mesoporous silica supported clay nanomaterials offer suitable solutions due to their large surface areas and precisely defined pore structures. It is known that Mt clay, obtained by enriching bentonite, stands out with its high adsorption capacity and biocompatibility and has a promising position as a drug carrier. HPMC is a hydrophilic cellulose derivative widely used in the pharmaceutical industry, increasing the potential of Mt clay for controlled-release drug formulations. TMZ chemotherapy, which is frequently used in the treatment of glioblastoma, is usually applied together with standard treatment protocols including maximal surgical resection. TMZ is also can be used for breast cancer, melanoma and non-small-cell (NSCL). It is known to be widely used in other types of cancer, such as lung cancer (for example, NSCL), but it may or may not be associated with glioblastoma. Although it improves the survival rates of cancer patients, TMZ is known to be limited by rapid clearance, low solubility, and undesirable side effects. Therefore, the main aim of this study was investigating the controlled release of TMZ through HPMC-modified Mt clay. The purification process of Mt clay involves mineral enrichment techniques, allowing the material to be checked for quality and suitability

for pharmaceutical applications. The enrichment process was carried out by purifying Mt clay from non-clay minerals by sedimentation method and aimed to separate clay particles with sizes below 3-5 micrometers. After enrichment, raw and purified Mt samples were comprehensively characterized using various analytical techniques. X-ray diffraction (XRD) technique was used to analyze the crystal structure, X-ray fluorescence (XRF) spectroscopy to determine the elemental composition, scanning electron microscopy (SEM) for surface imaging, and transmission electron microscopy (TEM) to examine the morphological structure. Surface areas of clay mineral samples were determined using the BET (Brunauer- Emmett-Teller) N_2 sorption technique. Zeta potential and particle size analyzes were also performed to evaluate surface charge and particle size distribution. Loading TMZ ingredient into enriched Mt was performed as described follow. First, 150 mL of TMZ solution was added to various Mt and HPMC compositions to prepare six different drug formulations. Each formulation was incubated on a magnetic stirrer at 37°C for 24 hours, then dried at 37-40°C. The dried mixtures were then turned into powder form using a agate mortar. To determine the concentration of TMZ in solutions, TMZ solutions of different concentrations were prepared. Spectra within the wavelength range 200-400 nm were then recorded and the wavelength at which the TMZ exhibited the most prominent absorbance peak was determined as 289 nm. Formulation's TMZ release profiles were evaluated in simulated gastric fluid. For this, each capsule from each formulation was added into dialysis bags containing simulated gastric fluids, and then each dialysis bag was placed in release media. While the stirring process was continuing by magnetic stirrer, samples were taken from the aqueous media at certain time intervals and TMZ concentration measurements were made with a UV spectrophotometer at 289 nm wavelength, and thus TMZ release amounts were determined against time. According to the data obtained from TMZ release profiles, a rapid release started in the first 15 minutes in all drug formulations except F1 and this rapid release continued for 45-60 minutes. Thus, at the end of 60 minutes, approximately 60-70% cumulative TMZ release was achieved. In the F1 formulation, rapid release continued for 90 minutes and cumulative TMZ release reached approximately 92%. The reason for the faster release in the F1 formulation is that the drug carrier system consists only of Mt clay, that is, there is no HPMC in the

formulation. It has thus been proven that HPMC molecules cause delayed release because they cover the surface of TMZ-loaded Mt clay. Again, it was determined that the F4 formulation exhibited a rapid release of TMZ since it did not contain HPMC. It was determined that TMZ release was slower as the HPMC ratio increased in the formulations. Another result obtained from the release profiles is that the carrier system and TMZ composition ratio change the release kinetics. It was determined that the release was slower in formulations with a TMZ/carrier system ratio of 1/5 compared to those with a 1/10 ratio. This can be explained by the fact that in 1/5 ratio formulations, the TMZ ratio is higher than the carrier system, which causes a higher driving force. Namely, it can be said that as the adsorbate (TMZ) concentration increases, the mass transfer between the clay layers becomes more intense and stronger. Thus, when the TMZ concentration is less than the amount of clay, adsorption mostly occurs on clay surfaces, while as the concentration increases, adsorption occurs on the surface and at the same time, intense adsorption occurs between the clay layers. During the drug release process, TMZ molecules accumulated between clay layers show slower release kinetics than molecules accumulated on the surfaces. According to the release profiles, it was seen that as the HPMC ratio increased, the cumulative TMZ release amount decreased slightly. As a result, it was determined that the F6 formulation showed the best controlled release kinetics. The F6 formulation exhibited rapid TMZ release of 50% levels in the first 45 minutes. In the following period, the release occurred more slowly for 360 minutes and reached approximately 90%.

2024, xiv + 81 pages

Keywords: Montmorillonite, Bentonite, Controlled drug release, Hydroxypropyl methylcellulose, Temozolomide.

ÖZET

Yüksek Lisans Tezi

HİDROKSİPROPİL METİL SELÜLOZ (HPMC)-MODİFİYE MONTMORİLONİT İLE TEMOZOLOMİTİN KONTROLLÜ SALIMI

Firoozeh PANAHIAN LARKEY
Afyon Kocatepe Üniversitesi
Fen Bilimleri Enstitüsü
Nanobilim ve Nanoteknoloji Anabilim Dalı
Danışman: Doç. Dr. Hakan ÇİFTÇİ

Bu çalışma, montmorillonit (Mt) kilinin potansiyel uygulamalarını hem doğal halinde hem de hidroksipropil metilselüloz (HPMC) ile modifiye edildiğinde kontrollü ilaç salımı için uygun bir aday olarak incelemektedir. Araştırmanın ana odak noktası özellikle glioblastoma tedavisi için kritik bir öğe olan temozolomid (TMZ) etrafında dönmektedir. Mezo gözenekli silika destekli kil gibi inorganik kompozit nanomalzemeler geniş yüzey alanları ve kesin tanımlı gözenek yapıları nedeniyle uygun çözümler sunar. Bentonitten zenginleştirilmesi ile elde edilen Mt kili yüksek adsorpsiyon kapasitesi ve biyolojik uyumluluğu ile öne çıkarak, ilaç taşıyıcısı olarak umut verici bir konumda bulunduğu bilinmektedir. HPMC farmasötik endüstride yaygın olarak kullanılan hidrofilik bir selüloz türevidir ve Mt kilinin kontrollü salım ilaç formülasyonları için potansiyelini arttırır. Glioblastoma tedavisinde sıkça kullanılan TMZ kemoterapisi, genellikle maksimal cerrahi rezeksiyonu içeren standart tedavi protokolleriyle birlikte uygulanır. TMZ'nin glioblastoma dışında meme kanseri, melanom ve non-small-cell lung (NSCL) kanseri gibi diğer kanser türlerinde de yaygın olarak kullanıldığı bilinmektedir, ancak glioblastoma ile ilişkili olabileceği gibi olmayabilir. Kanser hastalarının hayatta kalma oranlarını artırmasına rağmen, TMZ'nin hızlı temizlenme, düşük çözünürlük ve istenmeyen yan etkilerle sınırlı olduğu bilinmektedir. Bu nedenle, bu çalışmanın temel amacı, HPMC-modifiye Mt kil üzerinden TMZ'nin kontrollü salımını araştırarak bu sınırlamaları azaltmaktır. Mt kilin saflaştırma süreci, mineral zenginleştirme tekniklerini içerir ve bu, malzemenin

farmasötik uygulamalar için kalite ve uygunluk açısından kontrol edilmesini sağlar. Bu çalışma, Mt kilinin HPMC modifikasyonu ve kontrollü salım stratejileri arasındaki potansiyel sinerjiye odaklanarak ilaç salım sistemleri alanına değerli katkılarda bulunmayı amaçlamaktadır. Bu çalışma için, çoğunlukta Mt kilinden oluşan ticari bentonit cevheri zenginleştirme ve ilaç salımı çalışmaları için kullanıldı. Zenginleştirme süreci Mt kilinin sedimantasyon yöntemi ile kil dışı minerallerden arındırılması ile gerçekleştirildi ve kil partiküllerini 2 mikrometrenin altındaki boyutlarda ayırmayı hedefledi. Zenginleştirme sonrasında ham ve saflaştırılmış Mt örnekleri çeşitli analitik teknikler kullanılarak kapsamlı bir şekilde karakterize edildi. Kristal yapı analizi için X-ışını kırınımı (XRD), elementel kompozisyonun belirlenmesi için X-ışını floresansı (XRF) spektroskopisi, yüzey görüntüleme için taramalı elektron mikroskopisi (SEM) ve iç yapıyı incelemek için transmisyon elektron mikroskopisi (TEM) teknikleri kullanıldı. Kil mineral örneklerinin yüzey alanları (SBET), BET (Brunauer-Emmett-Teller) denklemi kullanılarak belirlendi. Ayrıca, yüzey yükü ve partikül boyut dağılımını değerlendirmek için zeta potansiyeli ve partikül boyutu da ölçüldü. TMZ'nin zenginleştirilmiş Mt'ye yüklenmesi için 150 mL TMZ çözeltisi, çeşitli Mt ve HPMC bileşimlerine eklenerek altı farklı ilaç formülasyonu hazırlandı. Her formülasyon, 37°C'de bir manyetik karıştırıcı üzerinde 24 saat boyunca inkübe edildi, ardından 37-40°C'de kurutuldu. Kuruyan karışımlar daha sonra bir havan kullanılark toz formuna getirildi. TMZ'nin çözeltide veya ilaç salım sonrasında konsantrasyonunu belirlemek için farklı konsantrasyonlarda TMZ çözeltileri hazırlandı. Dalga boyu aralığı 200-400 nm içindeki spektrumlar daha sonra kaydedildi ve ilacın en belirgin absorbans pikini sergilediği dalga boyu belirlendi. Formülasyonlardan TMZ'nin salım profilleri, simüle mide sıvısında değerlendirildi. Bunun için, her formülasyondan gelen her kapsül simüle mide sıvısı içeren dializ membranlara yerleştirildi. Bu diyaliz membranlar simüle mide sıvısı içeren beherlere yerleştirildi ve bir manyetik karıştırıcı üzerinde tutuldu. Karıştırma işlemi devam ederken belirli zaman aralıklarında sulu ortamdan örnekler alınarak 289 nm dalga boyunda UV spektorfotometre ile TMZ konsantrasyonu ölçümleri yapıldı ve böylece zaman karşı TMZ salım miktarları belirlendi. TMZ salım profillerinden elde edilen verilere göre F1 hariç tüm ilaç formülasyonlarında ilk 15 dakikada hızlı bir salım başlamış ve bu hızlı salım 45-60 dk boyunca devam etmiştir.

Böylece 60 dakikanın sonunda yaklaşık %60-70 kümülatif TMZ salımı gerçekleşmiştir. F1 formülasyonunda ise hızlı salım 90 dk boyunca devam etmiş ve kümülatif TMZ salımı yaklaşık %92 seviyelerine ulaşmıştır. F1 formülasyonunda daha hızlı salım sergilenmesinin sebebi ilaç taşıyıcı siteminin sadece Mt kilinden oluşması yani formülasyunun içeriğinde HPMC olmamasıdır. HPMC molekülleri TMZ yüklü Mt kilinin yüzeyini kapladığı için geciktirilmiş salıma sebep olduğu böylece kanıtlanmış oldu. Yine F4 formülasyonunda da HPMC olmadığı için hızlı bir TMZ salımının sergilendiği tespit edildi. Formülasyonlarda HPMC oranının artmasıyla birlikte TMZ salımının da daha yavaş olduğu belirlendi. Salım profillerinden elde edilen bir diğer sonuç ise taşıyıcı sistem ile TMZ bileşim oranının salım kinetiğini değiştirdiğidir. TMZ/taşıyıcı sistem oranın 1/5 olduğu formülasyonlarda 1/10 olanlara göre salımın daha yavaş olduğu belirlendi. Bu durum 1/5 oranlı formülasyonlarda TMZ oranın taşıyıcı sisteme göre daha yüksek olduğu ve bunun da daha yüksek itici güce sebep olduğu ile açıklanabilir. Şöyle ki, adsorbat (TMZ) konsantrasyonu arttıkça kil tabaka aralarına doğru olan kütle transferinin de daha yoğun ve daha kuvvetli olduğu söylenebilir. Böylece TMZ konsantrasyonu kil miktarına göre daha az iken adsorpsiyon çoğunlukta kil yüzeylerinde olurken, konsantrasyon arttıkça bir taraftan yüzeyde adsorplanma olurken aynı anda kil taba aralarında da yoğun şekilde adsorplanma gerçekleşir. İlaç salım sürecinde ise kil tabaka aralarında biriken TMZ molekülleri yüzeylerde biriken moleküllere göre daha yavaş bir salım kinetiği gösterir. Salım profillerine göre, HPMC oranının artmasıyla birlikte kümülatif TMZ salım miktarının da bir miktar düştüğü görüldü. Sonuç olarak, en iyi kontrollü salım kinetiğini F6 formülasyonunun gösterdiği belirlendi. F6 formülasyonu ilk 45 dakikada %50 seviyelerin hızlı bir TMZ salımı sergiledi. Devam eden sürede 360 dakika boyunca salım daha yavaş bir şekilde gerçekleşerek yaklaşık %90 seviyelerine ulaşmıştır.

2024, xiv + 81 sayfa

Anahtar Kelimeler: Montmorillonit, Bentonit, Kontrollü ilaç salımı, Hidroksipropil metilselüloz, Temozolomit.

APPRECIATION

I would like to thank my thesis advisor Assoc. Prof. Dr. Hakan ÇİFTÇİ for his great contributions to the subject of this research, directing the experimental studies, evaluation and writing of the results. I would also like to thank Asst. Prof. Dr. Muhammet Davut ARPA and my friends for their help, suggestions, and criticisms on every subject throughout the research and writing.

I would like to thank my family for their financial and moral support throughout this research.

Firoozeh PANAHIANLARKEY

Afyonkarahisar 2024

CONTENTS INDEX

Page

SYMBOLS and ABBREVIATIONS INDEX

Symbols

kg	Kilogram
min	Minute
Gy	Gray
G	Gram
nm	Nanometer
M	Molar
Mg	Miligram
mL	Mililiter
mm	Milimeter
mmol	Milimol
ppm	Parts per million
rpm	Revolution per minute
µL	Microliter
µm	Micrometer
µg	Microgram
ζ	Zeta potential

Abbreviations

3D-CRT	Three-dimensional conformal RT
5-Fu	5-Fluorouracil
AIC	5-amino-imidazole-4-carboxamide
BCNU	Carmustine
CCNU	Lomustine
BET	Brunauer-Emmett-Teller
CBTRUS	Central Brain Tumour Registry of the United States
CNS	Central Nervous System
CTAB	Cetyltrimethylammonium bromide
DNA	Deoxyribonucleic acid
DTAB	Dodecyltrimethylammonium bromide
DTIC	Dacarbazine
EG	Ethylene Glycol
EMA	European Medicines Agency
FDA	Food and Drug Administration
GBM	Glioblastoma
GFAP	Glial Fibrillary Acidic Protein
GRAS	Generally Recognized as Safe
H2O2	Hydrogen Peroxide
H2SO4	Sulfuric Acid
HCl	Hydrochloric Acid
HDTMA	Hexadecyltrimethylammonium chloride
HPMC	Hydroxypropyl methylcellulose
HTAB	Hexadecyltrimethylammonium bromide
IDH	Isocitrate Dehydrogenas
IHC	Immunohistochemistry
IMRT	Intensity-modulated R
LD50	Median lethal dose

MGMT	O6-methylguanine-DNA methyltransferase
MMR	mismatch repair machinery
MNP	magnetite nanoparticles
MRI	Magnetic resonance imaging
Mt	Montmorillonite
MTIC	meta-tyrosine or 5-(3-methyltriazol-1-yl) imidazole-4-carboxamide
N3MA	N3 Methyl Adenine
N7MG N7	Methyl Guanine
NCCN	National Comprehensive Cancer Network
NT	Nortriptyline
O6MG	O6 Methyl Guanine
ODTMA	Octadecyltrimethylammonium bromide
PLGA	Polylactic-co-glycolic acid
PPy	polypyrrole
ROS	Reactive Oxygen Species
SBET	Specific Surface Areas
SEER	Surveillance, Epidemiology, and End Results
SEM	Scanning Electron Microscopy
TBHDBP	Hexadecyltributylphosphonium bromide
TBP	Tetrabutylphosphonium bromide
TEM	Transmission Electron Microscopy
TMAB	Tetradecyltrimethylammonium bromide
TMZ	Temozolomide
VFX	Venlafaxine
WHO	World Health Organization
XRD	X-Ray diffraction
XRF	X-Rays fluorescence

FIGURES INDEX

Page

TABLES INDEX

Page

1. INTRODUCTION

Inorganic composite nanomaterials with extensive surface areas and well-defined pore structures have garnered significant interest due to their versatility and controllable pore characteristics. Significantly, the outstanding characteristics of mesoporous silica-pillared clays and porous nanoparticles based on silica encompass resilient thermal-chemical stability, an elevated surface area, and structures featuring micro-mesoporous qualities (Akhtar et al., 2014, Rodríguez-Garnica et al., 2019). These qualities render them invaluable for a diverse range of applications. For instance, they prove highly effective as adsorbents in separation techniques, capable of attracting and retaining other molecules on their surfaces. Furthermore, these materials serve as catalysts in chemical processes, accelerating chemical reactions (Liang et al., 2021, Pires, 2014). Additionally, they exhibit great potential as controlled-release delivery systems for active ingredients. This makes them particularly valuable for drug delivery, enhancing the effectiveness of treatments while reducing side effects (Yuan et al., 2021). Researchers have explored their application as drug delivery systems, yielding promising results (Ibrahim and Abdellatif, 2021). Overall, these nanomaterials, characterized by their expansive surface area and well-defined pore structures, offer a wide array of potential applications across various industries (Mandracchia and Tripodo, 2020).

Montmorillonite (Mt) clay, a pivotal component of bentonite, proves to be an incredibly versatile and multifunctional clay mineral. Its unique layered arrangement conforms to the overall chemical formula $(Na, Ca)_{0.3}(Al, Mg)_2 Si_4 O_{10} (OH)_2 \cdot nH_2O$, as described by Dekany and Lagaly (Bergaya and Lagaly, 2013). The negatively charged surface of Mt lends itself to attracting and binding positively charged molecules, such as drugs (Hassen et al., 2023). This mineral exhibits a plethora of remarkable properties that render it highly valuable across various applications. It boasts a high surface area, exceptional porosity, impressive adsorption capacity, biocompatibility, minimal to no toxicity, remarkable thermal and chemical stability, and an ability to remain resilient even in acidic environments (Lee et al., 2005). One of the standout qualities of Mt lies in its high adsorption capacity, which significantly enhances drug entrapment and the sustained release of drugs. In numerous formulations, Mt consistently upholds drug

release through strong drug absorption. Furthermore, it rapidly enhances the dissolution and bioavailability of hydrophobic drugs (Park et al., 2016). Mt serves as an effective encapsulation agent for drugs, safeguarding them from degradation and affording control over their release rates. In the production of advanced materials for pharmaceutical applications using Mt clay minerals (Joshi et al., 2009), the first stage entails eliminating gangue minerals, which comprise iron oxides, calcite, zeolite, mica, opal, feldspar, quartz, and other substances, from the raw clay. Diverse mineral beneficiation techniques like sedimentation, centrifugation, hydrocyclone separation, and chemical separation are favored for the purification of clay. (Carretero and Pozo, 2009). Given these exceptional qualities, Mt stands as an ideal candidate for advanced drug delivery systems within the pharmaceutical industry (Lee et al., 2005).

Hydroxypropyl methylcellulose, commonly known as Hypromellose (HPMC), is a hydrophilic cellulose derivative extensively utilized in the pharmaceutical industry to develop novel drug formulations for oral and mucosal applications, ensuring controlled release (Novak et al., 2012). This cellulose derivative possesses the unique quality of being water-soluble and electrically neutral, allowing for the creation of matrices that are both swellable and soluble (Khater et al., 2023). Additionally, HPMC solutions maintain stability in a pH range spanning from 3 to 11, and they resist enzymatic cleavage (Mašková et al., 2020). Notably, HPMC plays a crucial role in stabilizing amorphous pharmaceuticals through the formation of solid dispersions (Zhang et al., 2018).

In terms of safety, HPMC has gained acknowledgment as an approved excipient, designated as Generally Recognized as Safe (GRAS) by both the Food and Drug Administration (FDA) and the European Medicines Agency (EMA). It is accessible in the market under different trademarks, such as Metolose®, and Pharmacoat® (Shin-Etsu Chemical Company, Japan), Methocel® (Dow Chemical Company, MI, USA), as well as Benecel® (Ashland, The Netherlands) (Mašková et al., 2020). The HPMC molecule is comprised of a linear polysaccharide cellulose chain featuring hydroxypropyl and methoxyl side groups that are connected by ether links. Different types of HPMC display variations in their chemical composition, encompassing

differences in ratios and substitution degrees. These variances lead to distinctions in viscosity, particle size, and molecular weight (Naeli et al., 2020). This versatile polymer is extensively employed in the formulation of controlled-release dosage forms. Its mechanism involves swelling and forming a gel layer on the surface of matrix systems, effectively controlling the rate of drug release (Friuli et al., 2022). Notably, the non-ionic properties of HPMC reduce the likelihood of drug interactions and result in consistent drug release profiles, as the HPMC-based matrix is minimally affected by the pH of gastrointestinal fluids (Joshi, 2011). Overall, these characteristics establish the HPMC polymer family as the preferred choice for pharmaceutical excipients in the production of hydrophilic matrix-based dosage forms. HPMC offers a wide range of viscosity grades and a robust mechanism for drug release across various dosage forms. In summary, HPMC stands out as a versatile and indispensable polymer in the pharmaceutical field, particularly in the development of controlled drug release systems (Mašková et al., 2020).

Cancer emerges as a concerning issue on a global scale, contributing substantially to the mortality rate across the globe. Among the diverse forms of cancer, brain tumors present a particularly formidable challenge when it comes to diagnosis and treatment (Aldape et al., 2019). Glioblastoma (GBM), characterized as a grade 4 glioma (Louis et al., 2021), stands out as the most prevalent and deadliest brain tumor affecting adults, accounting for nearly half of all cases. The annual incidence of GBM is estimated to be in the range of 1 to 5 cases per 100,000 individuals, making it a relatively rare but devastating diagnosis. One of the most disheartening aspects of glioblastoma is its incredibly bleak prognosis. Patients diagnosed with GBM typically face a median survival period of only 15 to 18 months from the time of diagnosis. Shockingly, the five-year survival rate for GBM patients is less than 5%. This stark reality underscores the urgent need for improved treatment strategies and therapies in the fight against this aggressive brain cancer (Torrisi et al., 2022). In the realm of medical treatment, the gold standard for newly diagnosed glioblastoma patients involves the aggressive approach of maximal surgical resection of the tumor, provided it is feasible. Following surgical intervention, the administration of Temozolomide (TMZ) comes into play (Bush et al., 2019). This combined approach aims to maximize tumor removal while also utilizing

chemotherapy to target any remaining cancerous cells, striving to enhance patient outcomes and potentially extend survival periods.

Temozolomide (TMZ) is a potent alkylating agent utilized in glioblastoma therapy due to its ability to breach the blood-brain barrier. It functions as an oral alkylating agent, facilitating the transfer of alkyl groups to guanine bases, thereby inflicting damage to DNA (Iturrioz-Rodríguez et al., 2023). Unrepaired DNA damage can lead to apoptosis, or programmed cell death. The integration of this chemotherapeutic agent into the standard treatment for glioblastoma (GBM) followed a pivotal clinical trial in 2005, with subsequent trials confirming its effectiveness (Arakawa et al., 2021). The treatment procedure encompasses a blend of radiotherapy and TMZ, coupled with subsequent adjuvant TMZ, a combination proven to markedly elevate the median survival period of patients. When contrasted with solitary radiotherapy, this course of action extended the median survival from 12 months to 14 months. Additionally, there was a noteworthy enhancement in the survival rates of glioblastoma multiforme (GBM) patients at the 2-years mark, escalating from 10% to 26% (Iturrioz-Rodríguez et al., 2023). In addition to glioblastoma, temozolomide is widely used in another cancers such as melanoma (Iversen, 2013, Quirbt et al., 2007, Boogerd et al., 2007), non-small-cell lung cancer (Dziadziuszko et al., 2003, Iversen, 2013), and breast cancer (Trudeau et al., 2006), which may be associated with or without glioblastoma.

However, the efficacy of TMZ is hampered by several limitations. One key constraint is its short half-life, resulting in rapid elimination from the body. This rapid clearance can impede its ability to reach and eliminate cancer cells (Waghule et al., 2023). Additionally, TMZ exhibits poor solubility, posing challenges when it comes to dissolving it in water and, in turn, affecting its effectiveness. Another significant consideration is the drug's side effects. TMZ can induce adverse reactions such as nausea, vomiting, fatigue, and reduced blood cell counts (Jatyan et al., 2023). Despite these limitations, TMZ continues to offer a survival benefit for patients with GBM (Barrié et al., 2005, Arakawa et al., 2021) or other cancers such as melanoma (Iversen, 2013, Quirbt et al., 2007, Boogerd et al., 2007), non-small-cell lung cancer (Dziadziuszko et al., 2003, Iversen, 2013), and breast cancer (Trudeau et al., 2006), making it an indispensable treatment option for tumors. Researchers are persistently

exploring ways to enhance the drug's efficacy while minimizing its side effects (Iturrioz-Rodríguez et al., 2023, Stupp et al., 2009).

This study capitalizes on the remarkable attributes of Mt clay, such as its expansive surface area, cation exchange capacity, and swelling prowess, to address the imperative demand for controlled drug release in cancer treatments like TMZ. The principal aim of this study is to develop formulations that integrate unadulterated Mt clay with TMZ, alongside Mt clay that has undergone modification with HPMC. HPMC serves as a retarding agent, effectively postponing the release of TMZ and thereby enabling precise control over drug release. Notably, the investigation of TMZ release in conjunction with Mt clay marks a pioneering and previously uncharted domain of research. The use of Mt clay as a drug carrier has been explored in various studies, underpinned by its biocompatibility, biodegradability, and low toxicity. By introducing HPMC into the Mt clay-TMZ formulation, the controlled release of the drug is further optimized, rendering it a promising contender for cancer treatment.

To achieve this objective, Mt clay ores underwent an initial purification process employing mineral beneficiation techniques such as centrifuge-assisted gravity separation, flotation, and sedimentation. Following the characterization of the enriched and purified Mt clay, formulations involving various ratios of Mt and HPMC were prepared, with TMZ loaded into these formulations. The subsequent step involved measuring the release of TMZ in simulated stomach acid conditions at different time intervals.

2. CLAY MINERALS and MONTMORILLONITE

2.1 Overview and Categorization of Clay Minerals

Clay minerals, recognized for their stratified composition, are hydrated silicates of magnesium and aluminum. Their distinctive feature includes particle dimensions generally falling below 2 micrometers, and they encompass water crystalline within their structures. When heated, clay minerals display a remarkable plasticity, but they become solid when subjected to high temperatures. The crystal structure of clay minerals consists of layers, with tetrahedral (Si-O) and octahedral (Al-O-OH) layers stacked together and bonded by oxygen ions (as shown in Figure 2.1). These layered structures are categorized into two primary types: the 1:1 (TO) layer, which results from combining one octahedral layer with one tetrahedral layer, and the 2:1 (TOT) layer, formed by sandwiching an octahedral layer between two tetrahedral layers on either side (as depicted in Figure 2.2). The repetition of the tetrahedron-octahedron (TO) pattern gives rise to two-layered clay minerals, while the tetrahedron-octahedron-tetrahedron (TOT) pattern repetition leads to the formation of three-layered clay minerals. Clay minerals are commonly classified according to their layer structures and mineralogical traits, delineating various groups, including regular mixed-clays, 3 layers (T-O-T), and 2 layers (T-O) configurations. From a mineralogical standpoint, clays undergo further subdivision into distinct groups such as illite, chlorite, mica, smectite, kaolin, and attapulgite. Beyond mineralogical characteristics, clays can also be categorized based on diverse physical properties and their intended applications (Aboudi Mana et al., 2017, Ombaka, 2016).

2.2 Characteristics and Applications of Montmorillonite Clay

Montmorillonite clay, often known as bentonite, is an aluminum silicate with a layered composition in an aqueous form. It falls under the smectite group and exhibits a crystal

structure characterized by a monoclinic-prismatic arrangement. This structural configuration comprises an octahedral aluminum layer (O) positioned between 2 tetrahedral silicon layers (T), resulting in a T-O-T configuration (Ciftci, 2021). The surface of Mt clays carries a negative charge, a result of isomorphic displacements and cation coordination at the corners of the layers, which can vary in response to changes in ionic strength and pH within the suspension medium. To counterbalance this negative charge density, exchangeable cations like Na^{+}, K^{+}, Ca^{2+}, Mg^{2+}, and Al3+ insert themselves between the clay layers. The nomenclature of Mt clay varies based on the proportion of calcium and sodium ions within its layers, categorizing it into calcium montmorillonite, intermediate-type montmorillonite, and sodium montmorillonite (Bergaya and Lagaly, 2006, Bergaya and Lagaly, 2013).

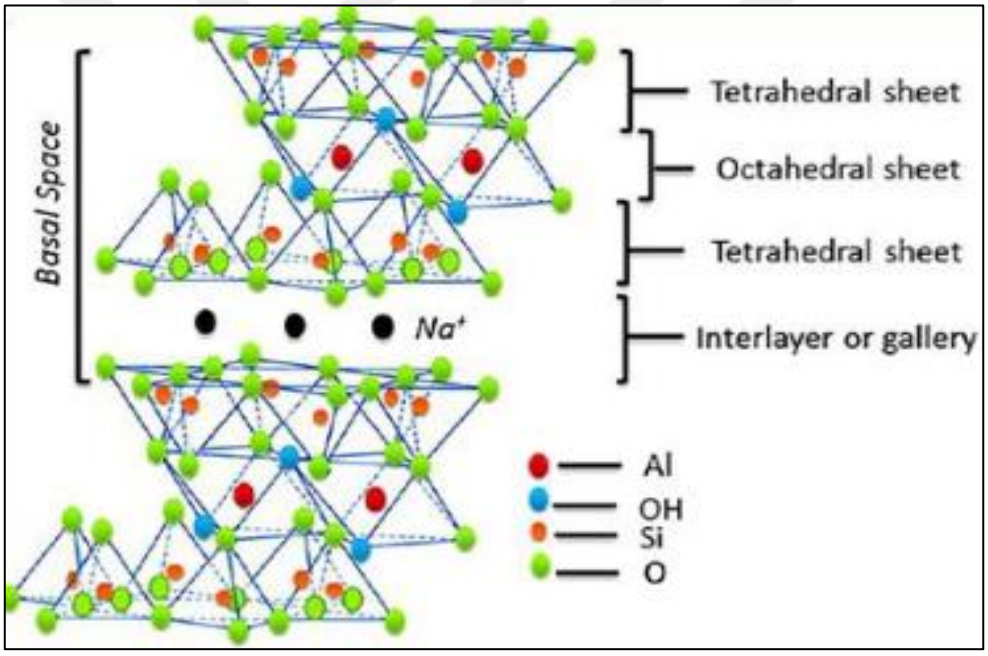

Figure 2.1 The crystal structure of clay mnerals: Octahedral layer and tetrahedral layer (Mokhtar et al., 2023).

Montmorillonite (Mt) clays exhibit outstanding attributes, such as an elevated surface area, exceptional adsorption capabilities, a high cation exchange capacity, mucoadhesive properties, non-toxicity, potent detoxifying abilities, oral biocompatibility, notable plasticity, swelling capacity, robust mechanical properties, and high chemical stability. Thanks to these attributes, Mt clays find applications across

a wide range of industries, serving as raw materials in construction, adsorbents, catalysts, food additives for aflatoxicosis prevention, antibacterial agents in dental and food packaging, lubricants in pill manufacturing, emulsifiers, components in drilling mud, and contributors to the ceramics field (Uddin, 2018). Due to their outstanding properties, Mt clays are promising candidates for inclusion in nanocomposite materials, especially in the development of next generation drug delivery platforms (Jayrajsinh et al., 2017).

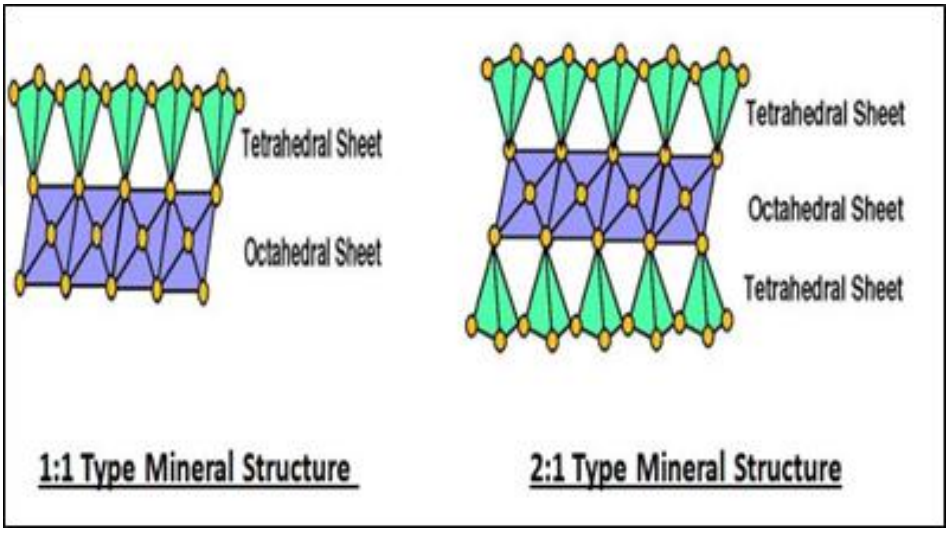

Figure 2.2 The categorazation of crystal structure of clay minerals: Clay minerals with 2:1 and 1:1 layer structures (Marchuk, 2016).

2.3 Role of Montmorillonite in the Pharmaceutical Industry

Clay minerals have a rich history of use for therapeutic and cosmetic purposes dating back to ancient times. Today, they continue to play a significant role in various pharmaceutical products. Mt clay, in particular, is a key focus of research in the pharmaceutical industry, with applications ranging from serving as an active ingredient to acting as a delivery system for other active components. The development of new nanocomposite materials combining active ingredients with clay minerals offers a range of crucial benefits, including controlled drug release, protection of active compounds, enhanced stability, and even targeted delivery of pharmaceuticals (Carretero, 2002, Carretero and Pozo, 2009, Yang et al., 2016).

Montmorillonite clay has secured its position in therapeutic applications due to its

remarkable capacity to adsorb microbial toxins, dietary toxins associated with gut issues, metabolic toxins linked to pregnancy, and hydrogen ions connected with acidosis. (Kryuchkova et al., 2021). It serves as a prevalent component in facial masks, efficiently eliminating oils and toxins from the skin surface owing to its substantial adsorption capacity. Moreover, it is advocated as an antiperspirant for inflammatory skin conditions such as ulcers, pimples, and boils, aiding in shine reduction and concealing blemishes (Carretero, 2002, Carretero et al., 2013, Choy et al., 2007, Kryuchkova et al., 2021).

Mt clay acts as an antacid by reducing gastric acid levels, as it can absorb excess protons in the stomach environment while releasing Mg2+ and Al3+ ions. Additionally, it serves as a gastrointestinal preservative by adhering to the stomach and intestinal membranes, fortifying the barrier, and reducing gastric and irritation secretions (Viseras et al., 2010). Table 2.1 outlines some of the therapeutic applications of Mt and other clay minerals.

Table 2.1 Therapeutic application of Mt and related clay minerals (Yang et al., 2016).

Mt and related clay minerals	**Applications**
Montmorillonite	Antidiarrheic
Talc	Pleurodesis (Fusion of Lung and Chest Membranes) Anti-Friction (Reducing Friction) Anti-Hemorrhoidal Antacid (Stomach Acidity Regulation) Antipruritic Gastrointestinal Protective Agent
Magnesium Trisilicate and Attapulgite	Antacid (Stomach Acidity Regulation) Antidiarrheal
Kaolinite	Homeopathic Remedy Gastrointestinal Protective Agent Antacid (Stomach Acidity Regulation) Anti-inflammatory Antidiarrheal

Several ongoing studies in the pharmaceutical industry are exploring the applications of Mt clay. One notable study, conducted by Wang and colleagues, focused on the development of a novel composite material consisting of Mt clay and polypyrrole (PPy).

This research aimed to investigate the loading and release characteristics of aspirin drug molecules. The outcomes of this study were promising, resulting in the creation of an innovative drug delivery system. This system demonstrates significant potential for use in drug release platforms, particularly due to its adjustable electric field. This adaptability is attained by capitalizing on the expansive surface area of Montmorillonite (Mt) clay and the electrical sensitivity characteristics of the graphene/polypyrrole material. Such advancements in drug delivery systems hold promise for enhancing drug release and control in pharmaceutical applications (Wang et al., 2016).

In a study conducted by Iliescu and colleagues, the researchers examined the release properties of the active ingredient irinotecan from a novel drug delivery system that incorporated Mt clay and sodium alginate. The findings revealed that this composite material exhibited continuous and controlled drug release when subjected to an environment simulating intestinal fluid. As a result, the authors proposed that Mt clay could serve as a viable alternative to systemic chemotherapy in the context of colorectal cancer (Iliescu et al., 2014).

Anirudhan and his team, delved into the controlled-release of paracetamol using a nanocomposite composed of Mt clay, chitosan, and MNP (magnetite nanoparticles). Their investigation revealed that the adsorption process of paracetamol onto the composite material adhered to the Sips model and displayed multi-layer adsorption behavior. Moreover, the prepared composite displayed a noteworthy swelling capacity, making it suitable for controlled and targeted drug release (Anirudhan et al., 2014).

In a research study by Jain and Datta, new nanocomposites were developed by combining PLGA (polylactic-co-glycolic acid) and Mt clay for drug delivery purposes. *In vitro* release results demonstrated that while the Mt free platform released approximately 60 precent of the drug within 30 hours, the carrier system with the addition of Mt clay exhibited controlled release over 25 hours, with drug molecules reaching close to 100% release (Jain and Datta, 2015).

A separate study focused on crafting a hybrid material by combining montmorillonite

with poly(l-lactide) to serve as a carrier platform for antidepressant agents. In this investigation, a micronized hybrid material was obtained by coating Mt clay with poly(l-lactide). The antidepressant drugs Nortriptyline (NT) and Venlafaxine (VFX) were absorbed within the layers of the clay. Results from the drug release experiments indicated that both medications exhibited a regulated release extending over a span of 20 hours (Rajkumar et al., 2015).

In a notable study, researchers delved into the creation of an innovative topical ocular delivery system intended for the treatment of glaucoma. The conventional approach of using eye drops to treat glaucoma encounters limitations related to rapid clearance from the ocular surface, which leads to a brief preocular residence time and diminished bioavailability. In response, the investigators devised nanoparticles for an ocular-controlled topical drug delivery system. These nanoparticles incorporated the BH drug within the layered gallery of Na-montmorillonite, further encapsulating chitosan nanoparticles. The resulting nanoparticles carried a positive charge and had an average diameter of 460 nm. Assessment through stimulation tests on human immortalized corneal epithelial cells and chorioallantoic membrane-trypan blue staining demonstrated their favorable tolerance for ocular tissues. A blood drug study revealed that the nanoparticles extended the retention time compared to a BH solution, indicating heightened bioavailability. This study underscores the potential of montmorillonite/chitosan nanoparticles as a promising alternative to traditional eye drops for glaucoma treatment (Li et al., 2018b).

A different investigation concentrated on creating and assessing mesoporous nanocomposites consisting of montmorillonite and magnetite loaded with 5-Fluorouracil. Using the sol-gel method, researchers synthesized these nanocomposites and employed various characterization techniques. Analysis of the drug release behavior from these nanocomposites revealed a sustained release pattern. This study underscores the potential of mesoporous montmorillonite/magnetite nanocomposites loaded with 5-Fluorouracil as a promising drug delivery system for cancer treatment (Çiftçi et al., 2020a).

2.4 Impact and Safety of Montmorillonite on Human Health

Before considering the utilization of clay minerals in pharmaceuticals or as drug carrier systems, it is of utmost importance to thoroughly understand their potential for harm and toxicity. The influence of mineral particles on human health can be significantly altered by variations in their shape, size, and mass concentration. Therefore, when conducting biological studies, it is essential to assess their pathogenic effects while maintaining control over these three crucial parameters. Mineral particles have the potential to induce two distinct types of diseases in humans. The first is silicosis, a condition stemming from exposure to quartz particles. The second, and far more severe, is asbestosis, a grave ailment resulting from the inhalation of asbestos particles (Carretero et al., 2013, Carretero, 2002).

Asbestos refers to mineral powders with a fibrous structure that can result in lung fibrosis, potentially leading to cancer and mesothelioma—a malignant lung membrane tumor. When producing advanced materials for the pharmaceutical industry using Montmorillonite (Mt) clay minerals, it is crucial to eliminate impurities like silicates, carbonates, iron oxides, aluminum oxides, minerals from the feldspar group, and organic substances from the raw clay ores. Numerous studies have been undertaken to evaluate the toxicity of Mt clays after their purification through diverse mineral preparation and enrichment methods (Carretero and Pozo, 2010).

Baek et al. conducted a study to evaluate how Montmorillonite (Mt) clay affects cultured cells. The results showed that concentrations above 100 μg/mL of Mt clay significantly inhibited cell proliferation during a 24 to 72 hours incubation. Notably, considerable cytotoxicity was observed only at a high dose of 1000 μg/mL after 48 to 72 hours. Importantly, the study found that Mt clay did not trigger the production of reactive oxygen species (ROS) at a dose of 500 μg/mL within a 24 hours incubation. The cytotoxicity of Mt clay was attributed to its small micronized particle size, impacting cultured cells by covering their surfaces rather than penetrating the plasma membrane. Furthermore, the research noted no in vivo toxicities, such as abnormal behaviors, symptoms, or body mass loss, during a 14 days oral administration study in

rats. The LD50 value of Mt clay was determined to be above 1000 mg/kg, indicating its non-toxic nature at practical doses, typically less than 100 mg/kg, in biological applications (Baek et al., 2012).

In a separate investigation, toxicity evaluations were performed on a nanocomposite material composed of Montmorillonite (Mt) clay and chitosan, developed as a carrier system for the anticancer drug 5-Fluorouracil (5-Fu). The study focused on genotoxic effects, employing Comet analysis in a human lymphocyte cell culture. Notably, a substantial decrease in DNA damage was observed when the drug was intercalated with Mt clay and integrated into the composites (Kevadiya et al., 2012).

In an independent investigation focused on drug release experiments utilizing Montmorillonite (Mt) clay with the anticancer drug 5-Fluorouracil (5-Fu), the potential toxicity of Mt clay on yeast models and rodents was explored. Biochemical analyses consistently yielded normal results in all histochemical examinations, confirming the non-toxic nature of Mt clay. Furthermore, histopathological evaluations of rodent tissues remained within standard parameters. Hematological tests on rodents led to the conclusion that Mt clay, when used in isolation, exhibits a wide range of non-toxic applications for both S. cerevisiae and Wistar rats (Lee et al., 2005).

In a sequence of research experiments involving Caco-2 cells and a nanocomposite material composed of a chitosan polymer and Montmorillonite (Mt) clay, thorough in vitro biocompatibility evaluations were carried out to assess the cytotoxicity and cell growth characteristics of this nanocomposite. The results of these assessments revealed that the Mt-chitosan hybrid material demonstrated biocompatibility within the concentration range of 5 to 500 μg/mL, concurrently exhibiting an efficient stimulation of cell proliferation (Salcedo et al., 2012).

Moreover, a study has indicated that Montmorillonite (Mt) clay particles do not accumulate in organs after entering the body, as supported by research conducted by Yang et al. (Yang et al., 2016) and Lal and Datt (Lal and Datta, 2015). Considering the results of this study, it is reasonable to assert that Mt clay can be utilized safely in

various pharmaceutical applications.

3. METHODS for PURIFYING CLAY MINERALS

Clay deposits frequently contain non-clay minerals like illite, zeolite, mica, feldspar, calcite, opal, and quartz, which can relegate certain clays to the category of low-quality materials. Improving the quality of these low-grade clays is crucial and indispensable because they may not be suitable for specific applications, such as nanocomposites, food, cosmetics, and pharmaceuticals (Eskanlou and Huang, 2021). Numerous beneficiation methods have been documented, encompassing processes such as sedimentation-centrifuge, ion exchange reactions, modification-centrifuge, stepped hydrocyclone, and chemical decomposition (Otunola and Ololade, 2020). When clays are destined for delicate applications like pharmaceuticals, food, and cosmetics, prompt washing is essential after the chemical beneficiation process. However, solid-liquid separation techniques, including centrifugation, evaporation, or filtration, pose challenges and expenses, especially in the context of clays. Therefore, whenever possible, it is recommended to prioritize cost-effective physical methods for obtaining pure clay materials (Eskanlou and Huang, 2021, Asamoah et al., 2018). The following section provides a summary of the clay beneficiation techniques employed in the industry.

3.1 Sedimentation

Sedimentation is a widely employed method in clay beneficiation, aimed at isolating pure clay minerals from other minerals like gangue minerals (quartz, feldspar, calcite, mica, etc.), which persist in larger particle sizes. These gangue minerals cannot be separated from clay minerals by relying on differences in specific gravity because their specific gravity values are quite similar. During sedimentation, clay minerals, characterized by considerably smaller particle sizes, remain in suspension, while the larger gangue minerals settle at the bottom. To prevent particle interactions during this process, it's crucial to maintain a solid ratio in the pulp around 0.5-1.0 wt.%. The time required for sedimentation is typically estimated using the Stokes sedimentation equation. An alternative equation for this estimation is given by t = 191.5 X/d^2. Physical purification processes rely on the difference in particle size between gangue and clay minerals. Gravity-based purification methods are ineffective due to the closely matched specific weights of gangue and clay minerals. Techniques for physical purification include sedimentation, centrifugal separation, aero separation, and sieving (Ciftci, 2021, Nieto et al., 2022).

3.2 Acid Leaching

The acid leaching technique is employed to augment the surface area and pore volumes of clay minerals, concurrently eliminating impurities and dissolving their outer layers. This method entails opening the crystal edges and substituting Ca2+ ions with H+ ions, thereby enhancing the catalytic properties of the clay. HCl (Hydrochloric acid) and H2SO4 (Sulfuric acid) are the most frequently used reagents for acid activation in this process. Crucial parameters such as the chemical composition of the clay, activation duration, acid concentration, and activation temperature induce alterations in both the chemical and crystal structure of the clay. Additionally, H2O2 (hydrogen peroxide) can serve as an oxidizing agent to eliminate organic substances from the clay (Ciftci, 2021, Kumar and Lingfa, 2020).

3.3 Flotation

Flotation is a mineral beneficiation method utilized for the separation of minerals based

on their distinct surface properties. In this process, hydrophobic minerals have a tendency to adhere to air bubbles formed within flotation cells and rise to the surface in aqueous media, while hydrophilic minerals tend to become wet and remain within the flotation cell. Clays, which can be challenging or even impossible to purify through alternative beneficiation methods, can undergo beneficiation via flotation. Given that most clays have inherently super hydrophilic surface characteristics, they are altered using surfactants (collectors) to render their surfaces hydrophobic before flotation. Additionally, non-clay minerals can also be modified through the application of various chemicals known as suppressors (Irannajad et al., 2019, Ozdemir and Çelik, 2010).

3.4 Centrifugal Beneficiation

Centrifugal beneficiation is a process that revolves around separating clay and non-clay minerals by leveraging the disparity in their particle sizes. It involves the utilization of equipment such as the Falcon gravity separator, Knelson gravity separator, multi-gravity separator, and hydro cyclones. Unlike the sedimentation method, this technique is more rapid and relies on centrifugal forces to achieve the separation of minerals, contingent upon variations in their specific gravity and particle size (Ciftci, 2021).

4. CLAY MODIFICATION

Clay minerals inherently possess hydrophilic properties and feature a negatively charged surface. This inherent nature limits their capacity to adsorb hydrophobic, nonionic, and cationic species. To surmount this limitation, clay minerals undergo various modification techniques. Acid activation and thermal modification are common methods used for clay mineral modification (Singla et al., 2012). Acid activation employs hydrochloric acid, sulfuric acid, or nitric acid to increase the surface area, porosity, and surface acidity of clay minerals. This process decomposes clay mineral particles, eliminates impurities, and dissolves outer surfaces. Bentonite clay (montmorillonite) is often activated using H_2SO_4 and is employed as a decolorizer in vegetable oils (Ismadji et al., 2015).

Thermal modification, on the other hand, entails subjecting clay minerals to different temperature ranges, leading to structural and compositional changes. The changes occur at specific temperature thresholds, including those below freezing (-5°C), temperatures above dehydration but below dehydroxylation, temperatures exceeding dehydroxylation but below structural destruction, and temperatures at which new phases are formed. The resultant changes are contingent upon the temperature range and the clay mineral type. Clay minerals modified through acid activation and thermal treatment exhibit enhanced adsorption efficiency, particularly in the remediation of contaminants such as dyes and

heavy metals in wastewater (Heller-Kallai, 2013).

Clay minerals possess inherent hydrophilic properties and negatively charged surfaces, which inherently limit their capacity for adsorbing hydrophobic, nonionic, and cationic substances. To circumvent these limitations, clay minerals undergo modification with surfactants to transform them from hydrophilic to hydrophobic organo-claysSurfactants are organic compounds identified by their polar heads and apolar hydrocarbon tails. They are classified as cationic, anionic, or nonionic surfactants depending on their water solubility (Xi et al., 2010).

While cationic surfactants like quaternary ammonium salts are prevalent in clay modification, nonionic surfactants offer their own advantages, such as biodegradability, non-toxicity, and excellent thermal and chemical stability. These modified clays, referred to as organo-clays, find applications across various industries, serving as adsorbents, fillers in polymer nanocomposites, rheology control agents in drilling fluids, and additives in paints and cosmetics (Sanchez-Martin et al., 2006). In the realm of surface modification studies, two key characterization techniques, hydrophobicity and zeta potential, prove invaluable in assessing the efficacy of the modification process.

Hydrophobicity is assessed by determining the contact angle between a solid surface and a water droplet, where higher contact angles indicate greater hydrophobicity. Zeta potential (ζ) measures the observable electric charge on the surface of solid particles, playing a vital role in comprehending and regulating dispersion-coagulation and adsorption processes (Fu et al., 2017). The efficacy of the modification process relies on the precise type and concentration of surfactants utilized. Therefore, it is crucial to ascertain the minimum quantity of cationic surfactant needed to achieve a hydrophobic or positively charged clay surface (Ismadji et al., 2015).

5. HYDROXYPROPYL METHYL CELLULOSE (HPMC)

Hydroxypropyl methylcellulose (HPMC), also known as Hypromellose, has evolved into a paramount hydrophilic cellulose derivative extensively utilized within the pharmaceutical industry (Figure 5.1). Its significance transcends as a key component in the formulation of innovative oral and mucosal matrix drug delivery systems designed for controlled release (Novak et al., 2012). Let's embark on a comprehensive exploration of this exceptional cellulose derivative, delving into its unique properties, diverse applications, regulatory accolades, and invaluable role in modern pharmaceutical formulations.

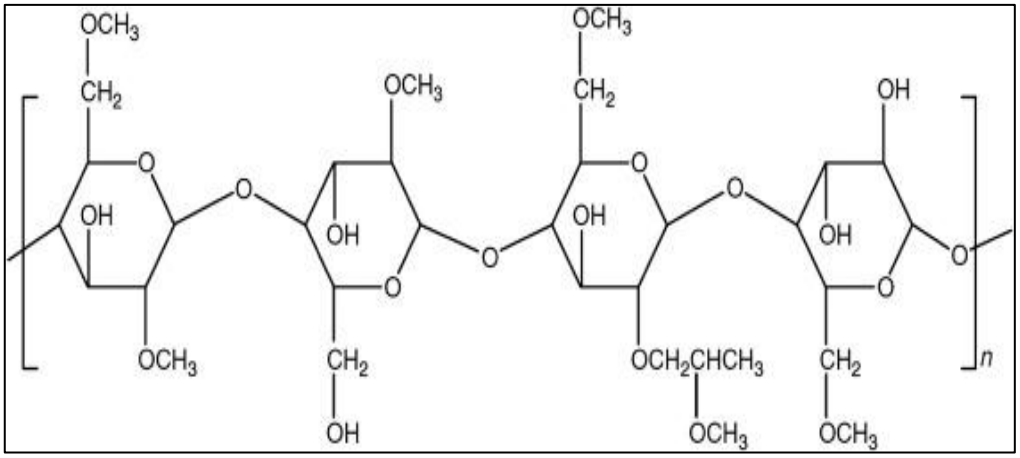

Figure 5.1 HPMC structure.

5.1 Innovative Properties

HPMC distinguishes itself with a set of remarkable properties that have captivated the pharmaceutical industry. At its core, it possesses the exceptional characteristic of being both water-soluble and electrically neutral, a rare combination that underpins its transformative capabilities. This distinctive quality empowers formulators to craft matrices that seamlessly blend swell ability and solubility, unlocking a new realm of possibilities in drug delivery (Khater et al., 2023).

5.2 pH Stability and Enzymatic Resistance

HPMC emerges as a versatile solution in drug formulations through its ability to maintain stability across a broad pH range spanning from 3 to 11. This stability is invaluable, especially in oral formulations where exposure to varying pH conditions is inevitable. Additionally, HPMC exhibits resistance to enzymatic cleavage, ensuring that the integrity of the pharmaceutical product remains intact, ultimately translating to enhanced therapeutic outcomes (Mašková et al., 2020).

5.3 Mastering Amorphous Pharmaceuticals

One of HPMC's notable contributions to the pharmaceutical landscape is its pivotal role in stabilizing amorphous pharmaceuticals. By orchestrating the formation of solid dispersions, HPMC safeguards the structure and efficacy of drugs. In an era where the bioavailability and therapeutic impact of medications are of paramount importance, this property is nothing short of revolutionary (Zhang et al., 2018).

5.4 Regulatory Recognition

From a regulatory standpoint, HPMC enjoys a laudable status as a permissible excipient. Both the Food and Drug Administration (FDA) and the European Medicines

Agency (EMA) have endorsed HPMC as "Generally Recognized as Safe" (GRAS). This distinction underscores the safety and suitability of HPMC for integration into pharmaceutical products, further solidifying its role in modern medicine (Mašková et al., 2020). It is commercially available under various trademarks, including Benecel® (Ashland, Netherlands) Pharmacoat® (Shin-Etsu Chemical Company, Japan), and, as well as Methocel® (Dow Chemical Company, MI, USA), Metolose®.

5.5 Diverse Chemical Composition

HPMC's allure extends to its diverse chemical composition, characterized by variations in methoxyl and hydroxypropyl side group arrangements. This diversity results in distinctions in molecular weight, viscosity, and particle size among different types of HPMC. Pharmaceutical formulators benefit immensely from this array of options, allowing them to meticulously select the most appropriate HPMC variant for their specific drug formulations. It's akin to having a tailor-made solution for each pharmaceutical challenge (Naeli et al., 2020).

5.6 Mastering Controlled Release

HPMC takes center stage in the arena of controlled drug release. Its unique capacity to swell and form a gel layer on the surface of matrix systems translates to precise control over drug release rates. This feature is instrumental in ensuring that drug concentration remains consistent and avoids abrupt spikes that could lead to undesirable side effects. This sophisticated mechanism enhances patient compliance and safety (Friuli et al., 2022).

5.7 Non-Ionic Virtue and pH Neutrality

An outstanding feature of HPMC is its non-ionic nature, a quality that minimizes the potential for drug interactions. Furthermore, its behavior remains remarkably stable regardless of the pH levels within gastrointestinal fluids. This inherent pH neutrality assures that the drug reaches its intended target area while minimizing any adverse

effects on surrounding tissues. This is a paramount consideration in contemporary drug delivery systems (Joshi, 2011).

5.8 Viscosity Grades and Versatile Dosage Forms

HPMC caters to the needs of pharmaceutical formulators with a wide array of viscosity grades, ensuring that the most suitable grade can be chosen for each specific application. This adaptability extends to various dosage forms, including tablets, capsules, gels, and suspensions. HPMC's seamless integration into diverse formulations renders it an indispensable component in the pharmaceutical industry's arsenal (Mašková et al., 2020).

In conclusion, HPMC has emerged as a cornerstone of innovation in the pharmaceutical industry. Its versatility, unwavering safety, and unique properties make it a critical element in the development of advanced drug formulations. As pharmaceutical science continues to evolve, HPMC remains a dependable and versatile tool for formulators who seek precise control over drug release and aspire to achieve enhanced therapeutic outcomes. Its rich history, adaptability, and unblemished safety record have firmly established it as the polymer of choice for crafting hydrophilic matrix-based dosage forms, ensuring that pharmaceutical products continue to advance and improve the quality of patient care (Mašková et al., 2020).

6. DRUG RELEASE

Controlled release mechanisms have been utilized across various domains such as chemistry and dye (Langer and Peppas, 1983), cosmetic (Ammala, 2013), agriculture (Vejan et al., 2021), and pharmaceuticals (Tiwari, 2016). This method involves the gradual dispensing of a substance, ensuring a prolonged and consistent concentration within a medium. This stands in contrast to immediate release mechanisms (Zhang and Cresswell, 2015), as depicted conceptually in Figure 6.1 concerning drug molecules.

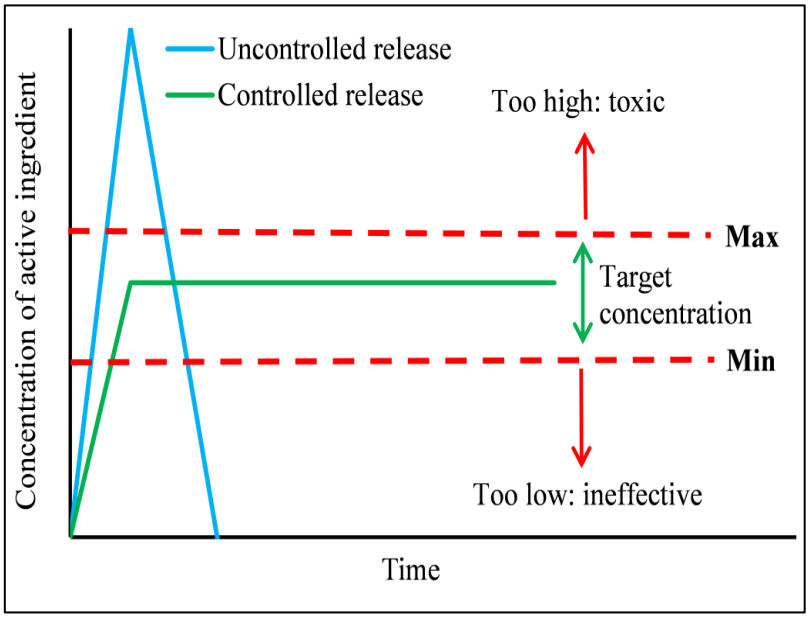

Figure 6.1 Diagram depicting the controlled release of medication.

6.1 Controlled Drug Release

The primary techniques for controlled release consist of delayed release, sustained release, and formulations for repeated action. Delayed release formulations retain drug compounds in the acidic gastric environment until they reach the neutral intestines. Sustained release formulations involve the immediate release of a portion of the drug, with the rest gradually dispensed over an extended period (usually 12 to 18 hours) (Wen and Park, 2010). Control over drug release is governed by three fundamental factors: the duration of drug release, the quantity of drug dispensed, and the location of drug release.

To attain the desired outcomes in pharmacotherapy, these three parameters must be effectively managed. The control of drug release depends on three crucial factors: the duration of release, the quantity dispensed, and the release location. Effectively managing these parameters is essential to achieve desired pharmacotherapeutic outcomes. Initiators such as pH levels (Yang et al., 2010, Wu et al., 2015), exposure to light (Li et al., 2018a), redox potential (Zhang et al., 2017), temperature (Im et al., 2009), and magnetic fields (Huang et al., 2009, Oliveira et al., 2013) are employed to activate controlled release mechanisms.

Unregulated drug release initially causes potentially harmful concentrations, followed by periods of inadequate drug concentration, posing significant health risks. This unpredictable pattern is linked to the inherent properties of the drugs and their mode of administration. Certain drugs exhibit short half-lives, resulting in swift elimination from the system and low plasma levels (Safdar et al., 2019). Controlled drug release formulations, like any other approach, possess their advantages and disadvantages, as detailed below:

Advantages:

- Maintenance of optimal drug concentrations, thereby extending the therapeutic

effects.

- Enhanced therapeutic efficacy with reduced drug quantities.
- Mitigation of side effects and reduced frequency of application.
- Improved patient comfort and compliance.

Disadvantages:

- In most cases, the drug's quantity in controlled-release forms exceeds that in single doses of conventional forms. If the controlled-release capsule is damaged, leading to the abrupt release of the drug, its concentration might surpass toxic levels.
- Once drug release commences, it's challenging to halt the process if necessary.
- The production cost of controlled-release formulations is typically higher compared to conventional forms.

7. GLIOBLASTOMA

Glioblastoma (GBM) is the most common primary brain tumor in adults, accounting for 45.2% of malignant primary brain and central nervous system (CNS) tumors. Unfortunately, GBM remains an incurable condition, with a median survival period of only 15 months (Thakkar et al., 2014). A mere 5.5% of patients survive for five years post-diagnosis. GBMs comprise both primary and secondary subtypes, each evolving through distinct genetic pathways affecting patients at different ages, leading to varying outcomes (Ostrom et al., 2016, Kleihues and Ohgaki, 2000). Primary GBMs constitute 80% of all GBMs and typically affect older patients, with an average age of 62 years. Conversely, secondary GBMs originate from lower-grade astrocytoma or oligodendroglioma, predominantly impacting younger patients, with an average age of 45 years. Secondary GBMs are commonly found in the frontal lobe, exhibit lower levels of necrosis, and generally offer a more favorable prognosis compared to primary GBMs. As defined by the WHO, GBM falls under the category of grade 4 cancer, characterized by its malignancy, mitotic activity, and predisposition to necrosis. Unfortunately, GBM is associated with an exceedingly bleak prognosis (Kleihues and Ohgaki, 2000, Urbańska et al., 2014).

7.1 Etiology and Epidemiology

Numerous genetic and environmental factors have been subject to investigation in the context of GBM. Yet, no risk factor accounting for a substantial portion of GBM cases has been pinpointed. Consequently, much like many other cancers, GBM is largely considered sporadic. However, one study did reveal a relatively high prevalence (17%) of prior therapeutic irradiation among GBM patients (Hodges et al., 1992). The latency period between irradiation and the onset of GBM varies, spanning from a few years to several decades. Some studies have explored the risk of GBM in relation to reduced susceptibility to allergies, immune factors, immune genes, and specific single nucleotide polymorphisms detected through genome-wide association studies (Wrensch et al., 2009).

These findings have indicated a lower risk of gliomas in individuals with allergies and atopic diseases (Brenner et al., 2002). Additionally, short-term use (less than 10 years) of anti-inflammatory medications has demonstrated a protective effect against GBM in certain studies (Scheurer et al., 2011). On the other hand, there is no substantial evidence linking GBM to lifestyle factors such as smoking, alcohol consumption, drug use, or exposure to N-Nitroso compounds (Hochberg et al., 1990). Investigations into the use of mobile phones have not indicated an increased risk of GBM development; however, the association with long-term usage requires further confirmation (Urbańska et al., 2014).

According to the 2013 report from Central Brain Tumour Registry of the United States (CBTRUS), the average annual age-adjusted incidence rate for GBM stands at 3.19 per 100,000 population. This places it as the highest incidence rate among malignant brain and central nervous system tumors. GBM predominantly affects adults, with a median age of diagnosis at 64 years. It is an exceedingly rare occurrence in children. Incidence rates climb with age, peaking between 75 and 84 years and gradually declining after 85 years. Given the aging population in the United States, an increase in the number of cases is anticipated (Urbańska et al., 2014, Ostrom et al., 2016, Ostrom et al., 2013). GBMs are more frequently reported in men, with an incidence rate 1.57% higher than

that of women (Ostrom et al., 2013). Primary GBMs are more common in men, while secondary GBMs are more prevalent in women (Ohgaki et al., 2004). Incidence rates of GBM are highest among white individuals, followed by black individuals. GBMs are most commonly observed in the supratentorial region and are exceptionally rare in the cerebellum and spinal cord (Urbańska et al., 2014).

7.2 Pathophysiology and Histopathology

Malignant cells demonstrate aberrant proliferation, growth, and angiogenesis primarily driven by mutations. In the case of GBM, a multitude of genetic and epigenetic mutations have been identified. The critical challenge lies in the identification and categorization of these mutations, a pivotal step in understanding the tumor's behavior and its resistance to treatment throughout the clinical trajectory.

The classifications delineate primary tumors originating from neural stem cell precursors and secondary tumors arising from mutations in mature neural cells, such as astrocytes. These genetic alterations result in deviations in gene expression and suppression compared to healthy brain cells. Consequently, these initiates both cellular and extracellular matrix modifications, giving rise to a diverse array of biochemical variations. This extensive genotypic diversity is encapsulated in the term "multiforme."(Olar and Aldape, 2014, Stoyanov et al., 2018). GBM manifests typical features of malignant tumors, such as the presence of atypical cells, nuclear hyperchromaticity, elevated mitotic figures, angiogenesis, and the occurrence of necrotic regions. Additionally, GBM displays heightened vascularity, with reports indicating that newly formed vessels may harbor multiple Weibel-Palade bodies—an attribute usually absent in brain endothelial cells. The presence of thrombi in these vessels may result in endothelial damage and subsequent proliferation (Linkous and Yazlovitskaya, 2011).

Two distinct patterns of necrotic regions have been identified in glioblastoma. One pattern exhibits a large necrotic area at the center, leading to inadequate blood supply, while the other comprises multiple small foci surrounded by pseudo-palisading. The

former is commonly linked to primary glioblastoma, whereas the latter is observed in both primary and secondary variants.

The classification of glioblastoma by the WHO (World Health Organization) encompasses both histopathological and molecular patterns. Histopathological categorization considers the presence of GFAP (glial fibrillary acidic protein) in astrocytoma, and the absence of GFAP expression signifies increasing malignancy and the presence of undifferentiated tumor cells. The molecular pattern is divided into IDH (isocitrate dehydrogenase)-mutant and IDH-wild type, detectable through IHC (immunohistochemistry).

The WHO morphologically categorizes tumors into grades I to IV. Grade I include benign tumors, grade II comprises relatively benign tumors, grade III involves low-grade malignant tumors, and grade IV is characterized by aggressive malignant tumors. Grade IV tumors, exemplified by glioblastoma multiforme, typically carry a median survival period of 6 to 12 months (Urbańska et al., 2014).

7.3 Diagnosis/Treatment/Management

MRI (Magnetic resonance imaging) by contrast enhancement serves as the primary diagnostic mode for GBM (Figure 7.1). At the point of diagnosis, research indicates that tumors typically fall within a 5-10 cm diameter range. GBM commonly extends into both occipital and temporal lobes bilaterally, involving the corpus callosum, producing a characteristic butterfly pattern in imaging. Hence, the colloquial term "butterfly glioma." To establish a definitive diagnosis, an intraoperatively removed tumor is subjected to histopathological examination. In situations where complete tumor resection proves unattainable or in suspected cases of metastatic GBM, fine-needle aspiration biopsy emerges as a viable option for accessible sites. A standard evaluation in such cases includes testing for specific markers such as GFAP, IDH mutation status, and O6-methylguanine-DNA methyltransferase (MGMT) promoter methylation status (Urbańska et al., 2014). The MGMT methylation status holds particular significance in predicting the response to specific chemotherapeutic agents. The development of a comprehensive treatment plan typically commences with maximal surgical resection,

followed by a course of chemoradiotherapy. (Urbańska et al., 2014).

Patient categorization is based on age, with distinctions between those over 70 and under 70. Each age category is further subdivided according to performance status, allowing for tailored treatment plans. In instances where patients are aged over 70 and exhibit a poor performance status, the consideration of hypo-fractionated radiotherapy as an alternative to the standard six-week course becomes relevant, particularly when coupled with chemotherapy. Treatment strategies may diverge for patients with methylated MGMT status, as they typically experience the most substantial benefits from temozolomide (TMZ), an alkylating agent. In such cases, the recommendation may not be for radiotherapy alone, although it could be contemplated for patients with unmethylated MGMT status. An array of conditions beyond GBM can yield abnormal imaging findings, including infectious, inflammatory, and demyelinating conditions, vascular malformations, strokes, benign tumors, and rare artifacts. This underscores the importance of a comprehensive diagnostic approach to differentiate between various potential causes of abnormal imaging results (Urbańska et al., 2014).

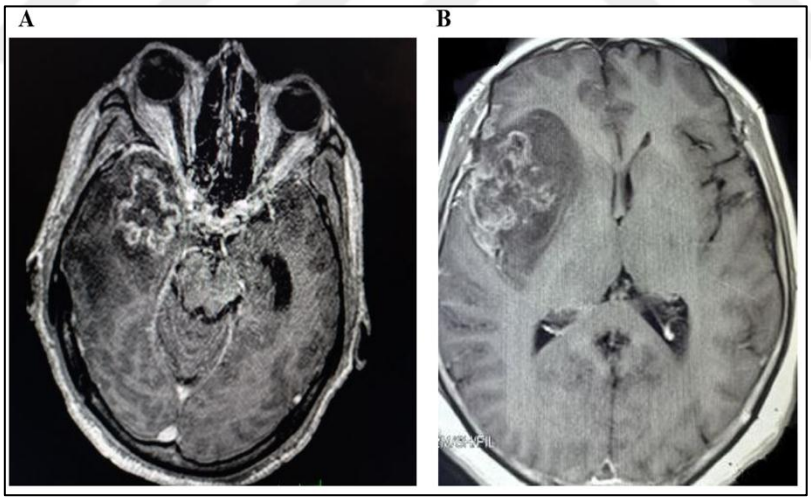

Figure 7.1 Temporal region GBM (A) and Peri-opercular GBM (B) (Urbańska et al., 2014).

The primary surgical goal is to attain the maximum safe resection while preserving neurological function and improving survival. Achieving complete removal is not always feasible due to the infiltrative nature of GBM. The SEER (Surveillance, Epidemiology, and End Results) program data indicates that both gross total resection and subtotal resection are associated with enhanced survival compared to no surgical

intervention or biopsy alone. The decision regarding whether to pursue subtotal resection, stereotactic biopsy, or palliative surgery depends on diverse factors such as the tumor's location, the patient's age, existing comorbidities, and individual patient preferences (Urbańska et al., 2014).

In the majority of cases, surgical resection plays a dual role, serving both as a definitive diagnostic procedure and a therapeutic intervention. Following surgery, it is customary to conduct a follow-up imaging assessment within 24-48 hours to evaluate the extent of the resection. The primary objective of radiotherapy is to administer radiation to the tumor and a margin of radiographically normal tissue, aiming to reduce the risk of recurrence. The conventional radiation dose entails the delivery of 50 to 60 Gy over a period of six weeks in 2 Gy fractions. Common methods for delivering radiotherapy include 3D-CRT (three-dimensional conformal RT) and IMRT (intensity-modulated RT) (Urbańska et al., 2014).

According to the guidelines of NCCN (National Comprehensive Cancer Network), the consideration of hypo-fractionated radiotherapy is suggested for patients with a diminished performance status or those aged over 70, regardless of performance status or MGMT promoter methylation status. Ongoing clinical trials are actively investigating the role of irradiation in recurrent GBM, with a pressing need for more comprehensive research addressing factors such as dose, frequency, fractionation, and prior treatments. As of now, radiation sensitizers, compounds utilized in conjunction with radiotherapy to augment its efficacy, lack approval for GBM. Adverse effects associated with radiation therapy encompass radiation dermatitis, neurocognitive toxicity, and potential future endocrinopathies (Urbańska et al., 2014).

Individuals undergoing simultaneous chemotherapy and radiotherapy face an increased susceptibility to developing leukopenia, thrombocytopenia, and hepatotoxicity. Vigilant monitoring, particularly through regular assessments like complete blood counts with differentials and liver function tests, is strongly recommended. In cases of severe thrombocytopenia, a temporary halt to radiotherapy might be necessary until blood

counts normalize. Considering the presence of lymphopenia, notably impacting CD4 counts, prophylactic measures for conditions such as pneumocystis pneumonia are advised for patients undergoing daily chemotherapy while concurrently undergoing radiotherapy (Urbańska et al., 2014, Arora and Somasundaram, 2019).

8. TEMOZOLOMIDE in GLIOBLASTOMA

Temozolomide (TMZ), functioning as a monofunctional DNA alkylating agent, holds a pivotal role in the clinical management of newly diagnosed GBM. The integration of TMZ regimens has markedly elevated overall survival and progression-free survival in comparison to radiotherapy alone, marking a significant advancement in GBM therapy. Possessing lipophilic properties, TMZ exhibits the capability to traverse the BBB (blood-brain barrier), and its stability under acidic stomach pH conditions allows for oral administration. The efficacy of TMZ is contingent upon a meticulously structured schedule; a singular higher dose proves ineffective, emphasizing the need for strict adherence to a specific regimen to attain desire outcomes (Urbańska et al., 2014, Arora and Somasundaram, 2019).

This alkylating antineoplastic agent is well-known for its potential for causing severe hematological toxicity and hepatotoxicity. TMZ is classified as a prodrug, and its active metabolite is meta-tyrosine (MTIC). It becomes active under neutral and alkaline pH

conditions. This drug falls into the Biopharmaceutics Classification System I category, boasting an impressive 100% oral bioavailability. It has a relatively short half-life of 1.8 hours, with peak concentration typically achieved within 0.5-1 hour. TMZ is commonly available in oral capsule form, with various brands like Deva, Koçak, Merck & Sharp, each containing five capsules per box. These capsules come in strengths of 5, 20, 100, and 250 mg, though it's worth noting that the 140 and 180 mg formulations have yet to receive approval in Turkey (Ünal et al., 2023). It's crucial to take TMZ on an empty stomach, approximately 30 minutes before a meal, and handle the capsules with bare hands. Treatment involving TMZ typically follows a 42-day cycle, with intervals and continuation for a specific duration. The capsule ingredients include anhydrous lactose, sodium starch glycolate, aerosil, tartaric acid, and stearic acid. In terms of solubility, it dissolves at a rate of 3 mg/mL in water, 22-25 mg/mL in DMSO, and 1 mg/mL in ethanol. Interestingly, TMZ's solubility remains consistent across different pH levels (Ahad et al., 2022, Krzak and Bilewicz, 2020).

Despite its benefits, the emergence of genetic or acquired resistance to TMZ inevitably leads to recurrence. Numerous clinical trials have explored the use of TMZ as a monotherapy for recurrent tumors, in addition to alternative therapies like CCNU (lomustine), BCNU (carmustine), and bevacizumab. However, none of these alternatives have demonstrated long-term benefits (Raizer et al., 2004, Yamamuro et al., 2021, Barrié et al., 2005).

The exclusive and conclusive indicator of TMZ resistance remains the MGMT promoter methylation status, despite various other resistance mechanisms documented in the literature. Most of these mechanisms either falter during clinical trials or remain untested. Our comprehension of GBM at the molecular level has undergone substantial expansion. Several crucial pathways and driving mutations have been pinpointed, presenting potential targets for treatment. Although many of these targets exhibited promise in animal models, their success did not translate into clinical efficacy, resulting in negligible improvement in patient survival.

A novel classification scheme for GBM has been introduced, incorporating molecular markers into histopathological grades. However, this classification lacks a strategy for stratifying patients based on TMZ response, except for those carrying IDH1/2 mutations, which forecast a favorable prognosis for low-grade gliomas and GBM. Consequently, GBM persists as a formidable challenge, eluding all endeavors to achieve a definitive cure (Sun and Turcan, 2021, Lin et al., 2021, Molenaar et al., 2018).

8.1 Temozolomide Chemistry and History

The drug development journey involves the creation of innovative chemical compounds and the thorough assessment of their viability as pharmaceutical agents. This procedure is intricate and time-consuming, with the ultimate objective being the provision of safe and efficacious treatments for patients. There exist two primary approaches in the drug development realm. The first entails the creation and assessment of a series of compounds to gauge their effectiveness against a range of diseases. The second method focuses on compounds specifically designed to target and inhibit a known disease-related mechanism. Remarkably, the trajectory of TMZ deviated from conventional routes, taking a distinctive and somewhat unconventional path after the initial synthesis of its precursors in the 1960s. Notably, the early testing stages were propelled by the dedicated efforts of a compact group of academic pharmacists (Arora and Somasundaram, 2019).

The journey commenced with the creation of imidazotetrazinone, a category of prodrugs generated through the reaction of diazonium with diverse isocyanates (Stevens and Newlands, 1993). The synthesis of TMZ originated from the combination of diazo-IC and methyl isocyanate. While several precursor compounds were explored subsequently, these two compounds emerged as the most effective for large-scale synthesis. In 1978, Robert Stone, an Aston University pharmacy graduate, collaborated with Malcolm Stevens during a student program with Plum and Baker Co., Ltd. Working alongside Eddy Lunt and Chris Newton, Stone played a pivotal role in crafting a bicyclic compound featuring an imidazole ring linked to a 1,2,3,5-tetrazine ring (Collins and Workman, 2006). Initially named Azolastone (a fusion of Aston and

Stone), it was later referred to as mitozolomide. Another Aston University student subsequently demonstrated its anti-tumor activity against leukemia and lymphoma in a mouse tumor model. In 1983, clinical trials were initiated by Aston University pharmacists involving this compound. However, due to its tendency for cross-linking, these trials faced setbacks, resulting in severe drug-induced thrombocytopenia (Lipinski and Hopkins, 2004).

Subsequent investigations unveiled a pivotal breakthrough in altering the toxicity profile of the compound by substituting a chloroethyl group with a methyl group in azolastone, leading to the emergence of a novel molecule known as TMZ. The TMZ initiative, backed by the pharmaceutical company Baker and May Ltd. and Cancer Research Campaign, successfully navigated financial challenges following the disappointment with azolastone. Ultimately, this endeavor resulted in the creation of TMZ, establishing its effectiveness as an anti-tumor medication for individuals with GBM. This accomplishment represents a noteworthy convergence of chemical and biological sciences in the fight against GBM (Arora and Somasundaram, 2019).

8.2 Mechanism Action of Temozolomide

Nearly a century ago, DNA alkylating agents were initially identified, originating from mustard gas developed and deployed during World War I between 1924 and 1928. Despite their use in chemotherapy since 1946, the precise mechanism of action involving DNA alkylation remained unknown until later. Notably, it wasn't until 1953 that the structure of DNA itself was unraveled (Arora and Somasundaram, 2019, Watson and Crick, 1953).

The alkylating agents most frequently employed for treating various tumor forms encompass dacarbazine, carmustine, lomustine, and TMZ. These drugs or their active forms produce methyldiazonium ions, characterized as electrophilic methylated species. Within the cellular milieu, DNA serves as a nucleophile, leading to the formation of multiple adducts. The characteristics, distribution, half-life, and cellular properties of these adducts govern the extent of cytotoxicity and the likelihood of resistance

development (Newlands et al., 1997, Zhang et al., 2012, Arora and Somasundaram, 2019).

Alkylating agents can be divided into two groups: mono-functional agents, which generate adducts with DNA, and agents causing biphasic cross-linking of DNA. TMZ falls within the category of mono-functional DNA alkylating agents and functions as a prodrug. It remains inert and stable under acidic pH conditions and achieves complete absorption upon oral administration. The hydrolysis of TMZ takes place under physiological pH, leading to the synthesis of MTIC (5-(3-methyltriazol-1-yl) imidazole-4-carboxamide). MTIC is subsequently subjected to hydrolysis, resulting in the production of AIC (5-amino-imidazole-4-carboxamide) and methyldiazolium. These compounds interact with DNA, liberating their methyl group in the process (Arora and Somasundaram, 2019, Newlands et al., 1997, Zhang et al., 2012). This sequence culminates in the generation of diverse DNA adducts (Refer to Figure 8.1).

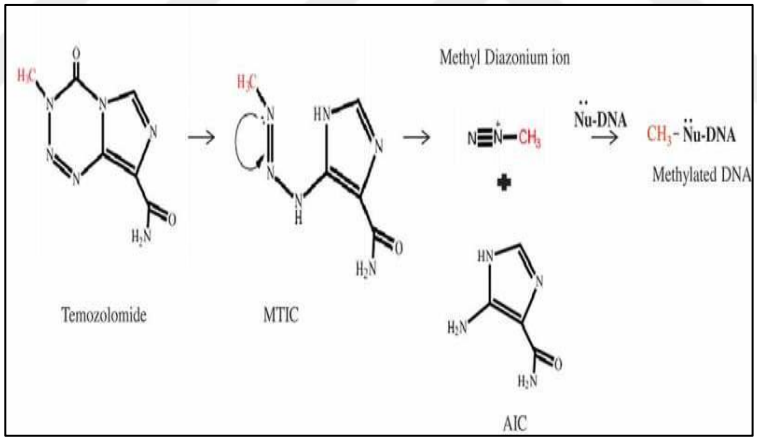

Figure 8.1 The mechanism of action of TMZ involves a chemical transformation.

8.2.1 DNA Adducts Formations

Formation of DNA adducts resulting from the reaction of DNA and temozolomide includes the following (Figure 8.2):

N7MG (N7 Methyl Guanine): The N7 position of guanine in the DNA structure stands out as the most nucleophilic site. This characteristic, stemming from its inherent nature

and accessibility in the major groove of DNA, designates it as the favored methylation site for temozolomide. As a result, N7MG constitutes approximately 70 percent of all adducts formed by temozolomide. Even though this adduct is prevalent in DNA, it does not disrupt the replication process or induce mismatches. Despite its high occurrence, the biological implications of this adduct remain uncertain. N7MG adducts are inherently benign, and their spontaneous depurination or enzymatic removal can lead to the formation of apurinic sites that are highly toxic to cells (Arora and Somasundaram, 2019, Newlands et al., 1997, Zhang et al., 2012).

N3MA (N3 Methyl Adenine): The N3 position of adenine within DNA serves as another highly nucleophilic site. Temozolomide induces the formation of a second type of lesion, N3MA, comprising 10% of the overall adducts. Similar to N7MG, N3MA does not induce mismatches but has demonstrated the ability to impede DNA polymerization in vitro. Notably, this blocking activity has been associated with N3MA generated by other alkylating agents, not specifically temozolomide. Additionally, N3MA has been observed to hydrolyze DNA under neutral pH conditions and physiological temperature, leading to the formation of abasic sites and the potential for cytotoxic effects (Arora and Somasundaram, 2019, Newlands et al., 1997, Zhang et al., 2012).

O6MG (O6 Methyl Guanine): O6 methylguanine, characterized as a weak nucleophile, manifests with a frequency of at least 5%. Despite its relatively lower occurrence, this lesion is the predominant factor contributing to the cytotoxic effects of temozolomide. O6MG forms mismatches with thymine, initiating recognition by the mismatch repair machinery (MMR). In the correction process, MMR removes thymine from the undamaged strand instead of eliminating O6MG. This results in the incorporation of additional thymidine during the replication process (Arora and Somasundaram, 2019, Newlands et al., 1997, Zhang et al., 2012).

Other alkylating agents have been reported to induce the formation of other methyl groups such as N3MG, N2MG, N7MA, and N1MA, but their relevance or association with temozolomide toxicity has not been established (Arora and Somasundaram, 2019,

Newlands et al., 1997, Zhang et al., 2012).

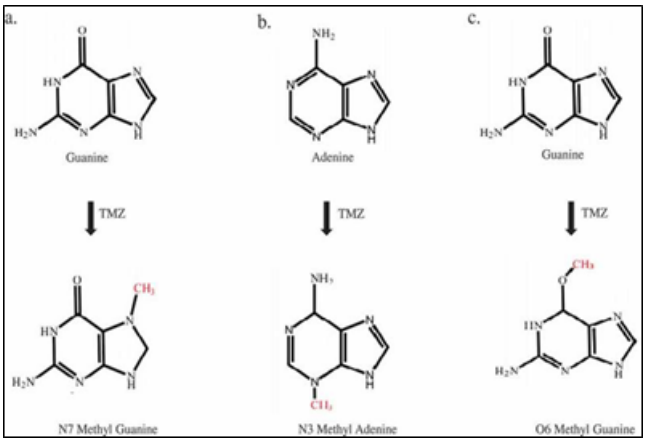

Figure 8.2 TMZ induces the formation of DNA adducts through its interaction with DNA, resulting in specific characteristics: A) N7MG (N7 methylguanine): Temozolomide methylates the N7 position of guanine. Upon exposure to temozolomide, around 70% of the adducts formed are N7MG. B) N3MA (N3 methyl adenine): Temozolomide methylates the N3 position of adenine. Approximately 10% of the adducts formed in cells exposed to temozolomide are N3MA. C) O6MG (O6 methylguanine): Temozolomide methylates the O6 position of adenine. About 5% of the adducts formed in cells exposed to temozolomide are O6MG. These adducts represent specific modifications to the DNA structure resulting from the interaction with temozolomide.

9. TEMOZOLOMIDE in OTHER CANCERS

Temozolomide is extensively utilized in various cancers alongside glioblastoma. It's employed in melanoma (Iversen, 2013, Quirbt et al., 2007, Boogerd et al., 2007), non-small-cell lung cancer (Dziadziuszko et al., 2003, Iversen, 2013), and breast cancer (Trudeau et al., 2006), either in connection with glioblastoma or independently. TMZ continues to provide survival benefits for patients with glioblastoma (Barrié et al., 2005, Arakawa et al., 2021) and other cancers like melanoma (Iversen, 2013, Quirbt et al., 2007, Boogerd et al., 2007), non-small-cell lung cancer (Dziadziuszko et al., 2003, Iversen, 2013), and breast cancer (Trudeau et al., 2006). This makes it an indispensable treatment option for various tumors. Researchers persistently seek ways to enhance the drug's effectiveness while reducing its side effects (Iturrioz-Rodríguez et al., 2023, Stupp et al., 2009).

9.1 Melanoma

Melanoma, despite constituting a minority of skin cancers, accounts for the majority of deaths associated with skin cancer. Mortality rate varies widely based on the stage of diagnosis. Early-stage melanomas have high survival rates, but advanced-stage melanomas significantly reduce life expectancy. Over recent decades, melanoma incidence rates have been steadily climbing worldwide, especially in regions with higher sun exposure. Factors contributing to this increase include greater awareness, increased UV exposure, and perhaps changes in diagnostic practices. It's crucial to note that melanoma incidence in younger adults has seen a particularly sharp rise. The primary cause of melanoma is UV radiation exposure, both from sunlight and artificial sources like tanning beds.

Mutations in genes responsible for regulating skin cell growth and repair, such as BRAF and NRAS, play a significant role in melanoma development. Moreover, individuals with fair skin, numerous moles, or a family history of melanoma are at higher risk. Alongside temozolomide, melanoma treatment involves surgery for early-stage tumors. For advanced stages or metastatic melanoma, immunotherapies like checkpoint inhibitors (such as pembrolizumab, ipilimumab) and targeted therapies (like BRAF inhibitors - vemurafenib, dabrafenib) have significantly improved survival rates. These therapies work by enhancing the immune response against cancer cells or targeting specific genetic mutations driving melanoma growth (Ahmed et al., 2020).

9.2 Non-Small-Cell Lung Cancer (NSCLC)

NSCLC stands as the most prevalent form of lung cancer and represents a leading cause of cancer-related fatalities worldwide. The overall prognosis for NSCLC remains poor, primarily due to late-stage diagnoses. While historically associated with smokers, the incidence of NSCLC among non-smokers is rising, possibly due to environmental factors like air pollution and exposure to secondhand smoke. It encompasses various subtypes, such as large cell carcinoma, adenocarcinoma, and squamous cell carcinoma, each exhibiting unique characteristics. Cigarette smoking is the leading cause of NSCLC, accounting for approximately 85% of cases. However, other factors like exposure to radon gas, asbestos, and genetic predispositions also contribute.

NSCLC tumors often have mutations in genes like EGFR, ALK, and KRAS, which guide treatment decisions. Treatment options for NSCLC depend on the stage and molecular profile of the tumor. Alongside temozolomide, chemotherapy, radiation therapy, targeted therapies (such as EGFR inhibitors - erlotinib, osimertinib) and immunotherapies (such as PD-1/PD-L1 inhibitors - pembrolizumab, atezolizumab) are used. Personalized medicine, guided by molecular testing of tumor tissue, is becoming increasingly important in determining the most effective treatment for NSCLC patients (Molina et al., 2008).

9.3 Breast Cancer (BC)

Breast cancer stands as a prominent cause of cancer-related fatalities among women worldwide, despite advancements in early detection and treatment that have contributed to improved survival rates over time. Incidence rates vary worldwide, with higher rates in developed countries. Age is a significant risk factor, with most cases diagnosed in women over 50, but breast cancer can also affect younger individuals. Genetic factors, hormonal influences, and lifestyle choices, such as alcohol consumption and lack of physical activity, contribute to its occurrence. Breast cancer is a complex disease with various subtypes, each with distinct characteristics and treatment implications. Hormonal factors (estrogen and progesterone receptors), HER2 gene amplification, and BRCA gene mutations are crucial in determining the subtype and guiding treatment decisions.

Treatment approaches for breast cancer depend on the subtype, stage, and individual patient factors. Alongside temozolomide, treatment may involve surgery (mastectomy or lumpectomy), radiation therapy, chemotherapy, hormonal therapy (such as tamoxifen), targeted therapies (like HER2-targeted drugs-trastuzumab, pertuzumab), and immunotherapy. Advances in precision medicine have led to more tailored treatments, improving outcomes for many patients (Smolarz et al., 2022).

10. AIM of STUDY

This study capitalizes on the exceptional properties of Mt clay, which include its expansive surface area, high caution exchange capacity, and remarkable swelling capabilities. These properties are harnessed to address the critical need for controlled drug release in cancer treatments, particularly in the case of TMZ. The main goal of this study is to create formulations that blend pure Montmorillonite (Mt) clay with Temozolomide (TMZ) and Mt clay modified with Hydroxypropyl Methylcellulose (HPMC).

HPMC serves as a crucial retarding agent, effectively delaying the release of TMZ. This allows for precise control over the drug release process. Notably, the investigation into the release of TMZ in combination with Mt clay represents a pioneering and previously unexplored area of research. The use of Mt clay as a drug carrier has been explored in various studies, driven by its remarkable biocompatibility, biodegradability, and low

toxicity. By introducing HPMC into the Mt clay-TMZ formulation, the controlled release of the drug is further enhanced, positioning it as a promising candidate for cancer treatment.

To achieve this objective, Mt clay ores underwent an initial purification process that employed mineral beneficiation techniques such as centrifuge-assisted gravity separation, flotation, and sedimentation. Following the characterization of the enriched and purified Mt clay, various formulations with different ratios of Mt and HPMC were prepared. TMZ was loaded into these formulations, and the subsequent step involved measuring the release of TMZ under simulated stomach acid conditions at different time intervals. This comprehensive research seeks to advance our understanding of controlled drug release mechanisms and their potential application in cancer treatment.

11. MATERIALS and METHODS

The study design comprised seven distinct steps, each of which is visually depicted in Figure 11.1 and 11.2.

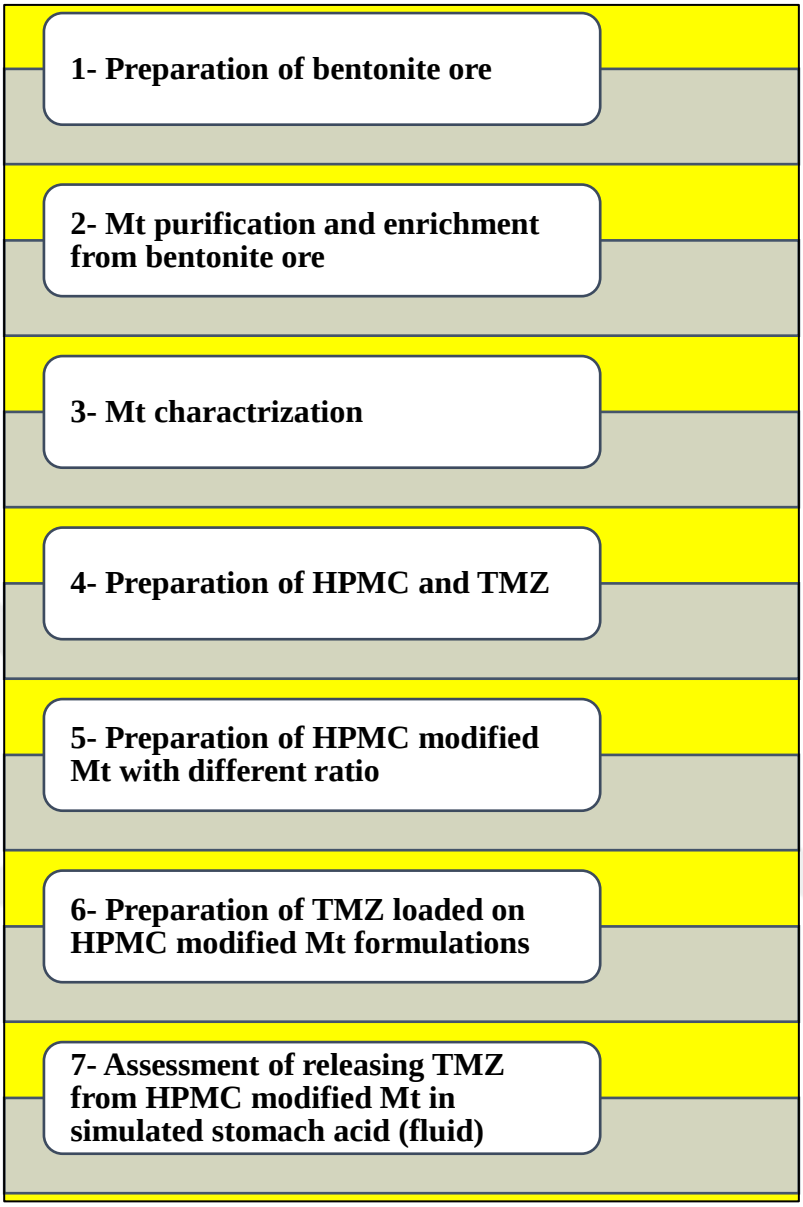

Figure 11.1 The seven distinct steps of study design.

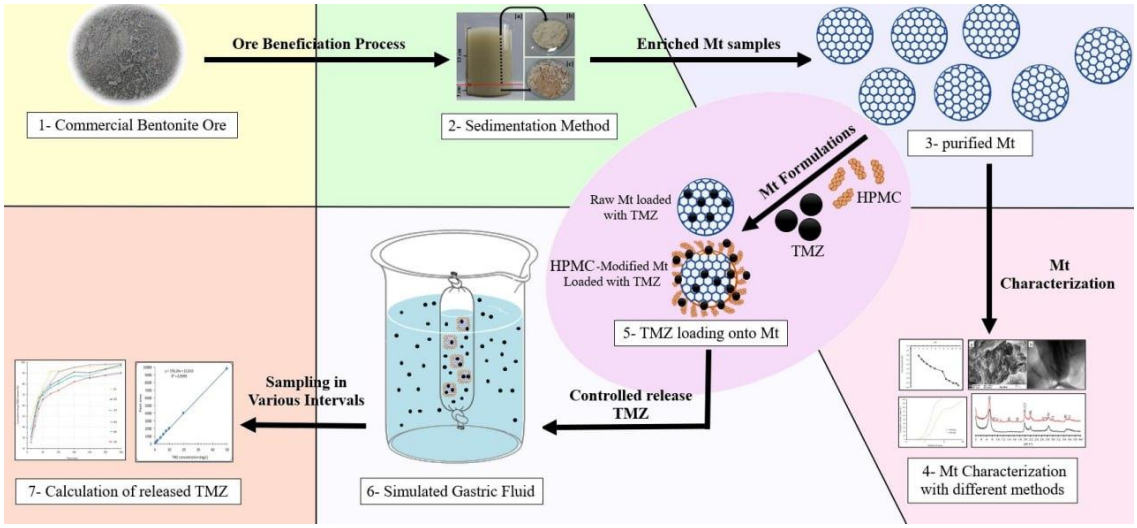

Figure 11.2 The study design comprised seven distinct steps: (1) Ccommercially bentonite ore was used as source of Mt. (2) The Mt purification and enrichment was performed by sedimentation method. The purified Mt (3) characterized with different methods such as XRD, XRF, SEM, TEM, zeta potential, specific surface areas, and particle size (4). (5) TMZ was loaded onto the HPMC-modified Mt and raw Mt clays. (6) Release profiles of TMZ from the formulated capsules were evaluated in simulated gastric fluid at various intervals. (7) Finally, calculation of released TMZ was conducted using a UV-visible spectrophotometer at 289 nm.

11.1 Materials

In this study, commercial bentonite ore containing predominantly Mt were used for clay purification, enrichment, organic modification, and drug release studies. The ore was obtained from Samaş Industrial Minerals, located in the Reşadiye-Tokat/Turkey region (Figure 11.3). This company is a market leader in Turkey and has been extensively researched in various studies, including preparation and characterization of organo-bentonites (Yeşilyurt et al., 2014, Hojiyev et al., 2016), the purification of bentonites (Yeşilyurt et al., 2014, Boylu et al., 2012), adsorption (Orucoglu and Haciyakupoglu, 2015), and preparation of clay-polymer nano-composites (Hojiyev et al., 2017). The properties and applications of additional chemicals employed in the experimental procedures are encapsulated in Table 11.1.

Table 11.1 The substances employed in the experimental procedures, along with their designated purposes.

Name	Formula	Brand	Applications
HPMC	C_2H_5OH, 99.7 %	Sigma	Polymer additive
Montmorillonite	$(Na, Ca)_{0.3}(Al, Mg)_2 Si_4O10 (OH)_2 \cdot nH2O$	SAMAŞ Industrial Materials	Drug carrier
Temozolomide	$C_4H_3FN_2O_2$, 99%	TLC	Active ingredient (drug) used in drug loading and release studies
Simulated gastric fluid	HCl 1N: 80 mL NaCl: 2 g Pure water: 420 ml pH: 1.2	Merck	Media used in drug release studies
Hydrochloric acid	HCl, 35-37%	Merck	Acid and bases used for pH adjustment
Sodium hydroxide	NaOH, 96%	Merck	

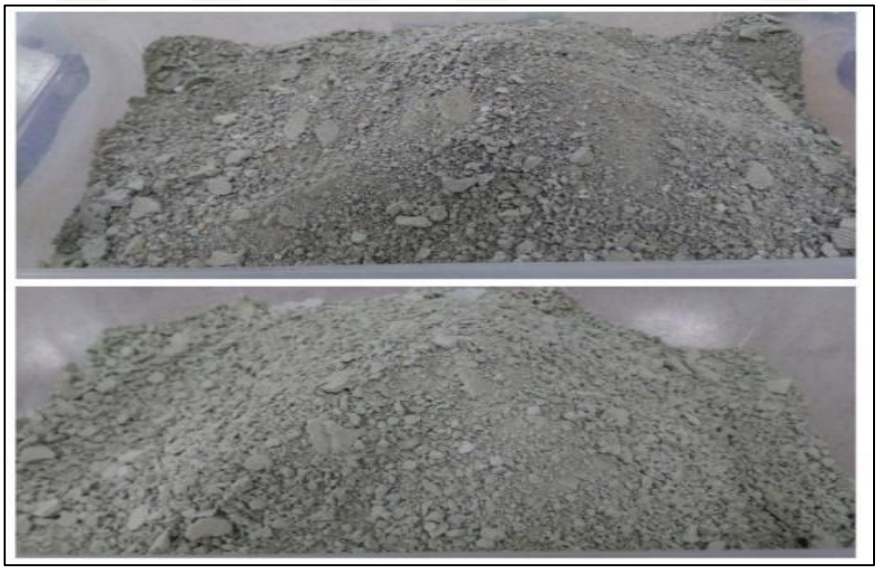

Figure 11.3 Air dried and crushed raw clay (bentonite) ore samples).

11.2 Montmorillonite Purification

The application of the sedimentation method aimed to achieve the refinement and enhancement of montmorillonite (Mt). In the sedimentation process, the primary objective is to segregate clay particles with dimensions below 2 micrometers, forming a colloidal system, from larger non-clay minerals settling at the bottom. This method enables the efficient separation of clay minerals from other constituents. To ensure optimal results and diminish particle interactions, it is essential to maintain the solid ratio in the pulp at approximately 1 percent. The sedimentation procedure encompasses several steps, detailed below in a systematic sequence:

1- Size Reduction: The raw Mt (bentonite ore) clays are initially reduced in size to particles under 5 mm. This size reduction is achieved using a jaw crusher followed by a roller mill. It's worth noting that sodium Mt readily disperses in water, obviating the need for additional crushing and grinding processes.
2- Clay Dispersion: After size reduction, 30 g of the clay sample is placed into three separate beakers, each containing 1 liter of pure water (Mt 10 g per beaker). The clay is left to disperse in the pure water for 24 hours. Afterward, it is mixed for 60 minutes at 1000 RPM using a mechanical mixer to ensure thorough dispersion.
3- Sedimentation Initiation: The sedimentation process begins, and it takes approximately 8 hours to allow for the complete settling of gangue minerals.
4- Decantation: To isolate the clay particles that have settled during sedimentation, the liquid above the precipitate is cautiously removed through decantation, ensuring that it is done up to a level of 3 cm from the top of the precipitate, as illustrated in Figure 11.4-a. This gradual siphoning process is employed to minimize the potential mixing of disrupted gangue minerals with the clay minerals, mitigating any turbulence effects.
5- Centrifugation: The siphoned clay particles are subjected to centrifugation for 12 minutes at 9000 RPM. This step helps in further separating the clay particles from any remaining impurities. The sediment pellet is collected and subsequently dried at 40°C.
6- Powder Collection: The dried powders, primarily composed of Mt, are then finely

ground in a mortar. These processed powders are collected and prepared for use in subsequent experiments (Figure 11.4-b).

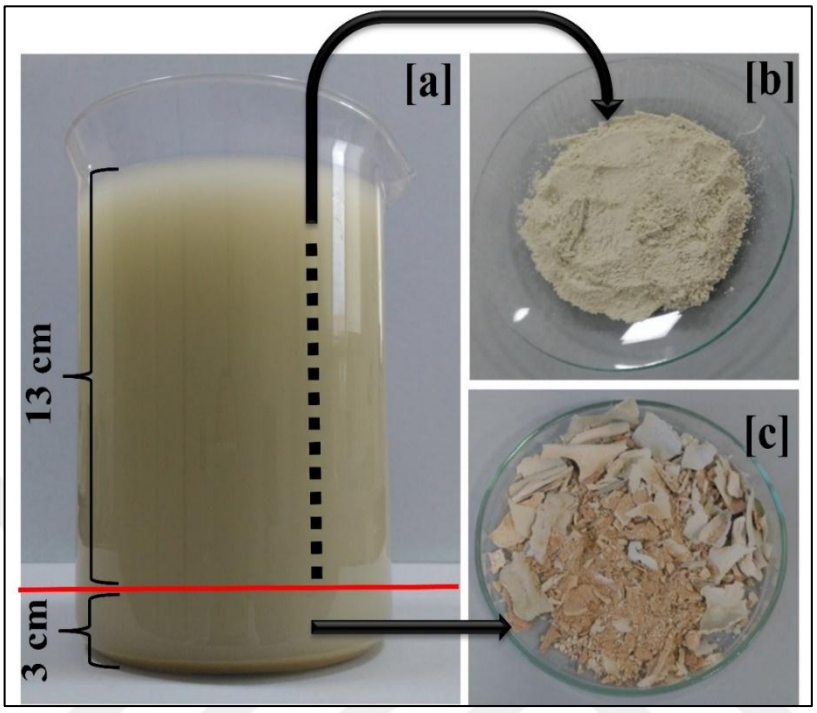

Figure 11.4 The sedimentation process depicted in images; (a) raw montmorillonite (Mt) dispersion, (b) sedimentation-treated Mt product, and (c) gangue minerals (Çiftçi et al., 2020b).

11.3 Montmorillonite Characterization

The raw and purified (enriched) Montmorillonite (Mt) samples underwent thorough characterization employing various analytical techniques. This encompassed XRD (X-ray diffraction) for the analysis of crystal structure, XRF (X-ray fluorescence) spectroscopy to determine elemental composition, SEM (scanning electron microscopy) for surface imaging, and TEM (transmission electron microscopy) to investigate the internal structure. The SBET (specific surface areas) of clay mineral samples were determined using the BET (Brunauer-Emmett-Teller) equation. Additionally, measurements of zeta potential and particle size distribution were conducted to assess the surface charge and size of the particles.

11.3.1 X-Ray Diffraction (XRD)

The raw and purified clay samples were allowed to air-dry for the assessment of their mineral composition. Subsequently, X-ray diffraction (XRD) patterns were obtained using a Shimadzu XRD-6000 instrument, operating at 40 kilovolts with Cu-Kα radiation (λ: 1.54174 angstrom). Scans were performed at a step speed of 0.02 degrees within an angular range of 2-70 degrees. For a comprehensive XRD analysis of oriented clay in Montmorillonite (Mt) samples, dispersions containing clay particles smaller than 2 μm were created through sedimentation.

A few drops of these clay dispersions were placed on glass slides and allowed to air-dry for one day, resulting in the preparation of three samples. Furthermore, one sample from each Montmorillonite clay was exposed to ethylene glycol vapor for two hours at 60 degrees Celsius, and another sample was heated at 550°C for 2 hours. Following this procedure, three samples were generated for each Mt clay sample, comprising air-dried, ethylene glycol-saturated, and 550 degrees Celsius-heated specimens. XRD analyses were carried out in the 2-20° range, as specified by Brown and Brindley (Brown and Brindley, 1980).

11.3.2 X-Rays Fluorescence (XRF) Spectroscopy

The samples underwent a drying process at 105 degrees Celsius for 24 hours, followed by a 2-minute milling procedure in a ring mill. Subsequent to this preparation, the chemical composition of both the raw and purified Montmorillonite (Mt) samples was analyzed using a Rigaku XRF device, model ZSX Primus II, facilitating elemental analysis.

11.3.3 SEM and TEM

The SEM (Scanning Electron Microscope) is a specialized electron microscope that produces images by scanning the surface of sample with a focused electron beam. Interaction between electrons and atoms in the sample generates signals containing crucial information about the sample surface's topography and composition. In this

research, SEM analysis was conducted using the device model of LEO1430 VP.

For a detailed analysis of the core-shell structure, particle shape, and particle size, a transmission electron microscope (TEM) of the JEOL brand, model JEM 2100F, was utilized. The analyses were performed at an accelerated voltage of 200 kilovolts. Sample preparation involved diluting them at a ratio of 1/20000 in ethanol and subsequently dispensing them onto a copper plate coated with carbon following ultrasound dispersion. Subsequently, the samples were allowed to dry under normal atmospheric conditions, after which they were placed in the holder for microscopy studies.

11.3.4 Surface Area and Pore Structure (SBET)

The SBET (specific surface areas) of the clay mineral samples were calculated using the BET (Brunauer-Emmett-Teller) equation. Furthermore, the pore size distribution was derived from the adsorption branch of the isotherm, employing the BJH (Bartrett-Joyner-Halenda) method. These measurements were conducted using a Micrometrics device, model Gemini 2360, which operates based on the adsorption and desorption of nitrogen gas. The gas adsorption isotherm, depicted in Figure 11.5, reveals distinct zones of gas pressure. In the low gas pressure range ($0 < P/P_0 < 0.2$), gas adsorption occurs primarily on particle surfaces and within micropores (with pore diameters between 0 and 2 nanometers.

As relative pressures increase ($0.4 < P/P_0 < 0.95$), multilayer adsorption takes place in mesopores (with pore diameters ranging from 4 to 40 nm). Finally, when relative pressures exceed 0.95, condensation begins in macropores (with pore diameters exceeding 40 nm). This information helps in understanding the porosity and surface characteristics of the samples.

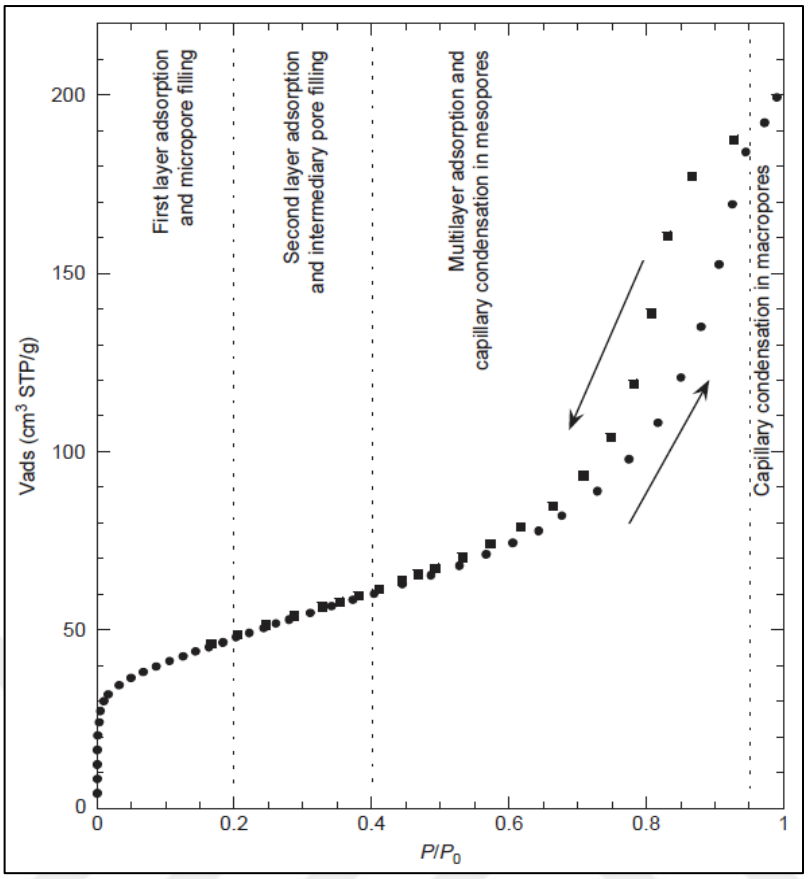

Figure 11.5 General representation of gas sorption isotherm (Michot and Villieras 2006).

11.3.5 Particle Size Distribution

The determination of particle size distributions was carried out using the Malvern Mastersizer 2000 instrument. To perform this analysis, dispersions obtained from sedimentation experiment was utilized. Here's a step-by-step description of the process:

1- Preparation of Analysis Chamber: A beaker with a volume of 1000 milliliters, filled with 800 milliliters of deionized water, was placed within the wet analysis chamber of the apparatus.
2- Background Reset and Mixing: Mixing was initiated at a speed of 2000 RPM, and a background reset procedure was conducted.
3- Sample Dispersion: Subsequently, the appropriate quantity of each sample was dispersed for a duration of 1 minute at 400 Watts, employing the Hielscher UP400S device.

4- Laser Obscuration: A specific volume of the dispersed samples was then gently introduced into the beaker until the laser obscuration reached a range of 3-6%.
5- Automatic Measurements: With laser obscuration within the desired range, automatic measurements were initiated. The analysis was repeated three times, and average values were recorded.

This process enabled the precise determination of particle size distributions for the samples under investigation. It is a crucial step in characterizing the physical properties of the materials, contributing valuable data for various research and industrial applications.

11.3.6 Zeta Potential

Zeta potential (ζ) serves as a measurable indicator of the electric charge present on the surface of solid particles when suspended in a liquid medium. This property plays a crucial role in defining the electrostatic repulsion forces around the particles, thereby influencing the overall colloidal system stability (Sondi et al., 1997). The analysis of zeta potential was carried out using the Malvern Nano-Z model zeta-meter device, involving several key steps:

1. Sample Preparation: Initially, samples underwent a drying phase at 105°C for 8 hours, followed by grinding for 2 minutes using a laboratory-scaled ring mill.
2. Sample Dispersion: Approximately 0.01 grams of the ground sample were introduced into a solution of 100 mL of 10^-3 M NaCl. The resulting mixture was dispersed using a magnetic stirrer.
3. Settling Phase: After 30 minutes of mixing, stirring was halted, allowing for a 5-minute interval during which coarser particles settled.
4. Sample Collection: A 1 mL sample was drawn from the dispersions using an injector and filled into the measuring cell.
5. Zeta Potential Calculation: Zeta potential values were automatically computed using the classical Smoluchowski formula, incorporating the measured electrophoretic mobility values of the particles. This process was repeated three times, and results

with a minimum standard deviation within the range of 3-5% were documented.

6. pH-Dependent ζ Measurements: To explore the pH dependence of the zeta potential, samples were prepared using solutions of 0.1-5 M HCl and 0.1-1 M NaOH. The pH values of these solutions were systematically adjusted within the range of 2 to 12.

These detailed zeta potential measurements offered critical insights into the electric charge characteristics of solid particles in different liquid environments, providing valuable information on the stability and behavior of colloidal systems under varying conditions.

11.4 Preparation of HPMC and TMZ

Before loading TMZ onto the Mt clays, we prepared solutions of TMZ and HPMC. To make the TMZ solution, we dissolved 200 mg of TMZ powder in 1000 mL of sterile distilled water on a magnetic stirrer, resulting in a 200 mg/ml drug solution. This solution was then stored at 4°C. For the HPMC work solutions, we warmed 100 mL of sterile distilled water, and gradually added 150 mg of HPMC powder on a magnetic stirrer until it dissolved. It's important to note that the solution should not be allowed to boil. The HPMC solution was left at room temperature until it dried into a gelatinous state.

11.5 TMZ Loading on HPMC modified Mt

The procedure for loading TMZ onto enriched bentonite (Mt) was carried out following the steps outlined in Table 11.2. In summary, 150 mL of TMZ solution was added to various ratios of Mt and HPMC, as specified in Table 11.2, resulting in the preparation of six different drug formulations. Each formulation was then incubated for 24 hours at 37°C on a magnetic stirrer. Subsequently, the mixtures were left at 37-40°C until they dried, after which they were ground into a powder form using a mortar and pestle. The resulting powder was then encapsulated into polymeric capsules, as depicted in Figure 11.6. For further testing, we prepared six capsules from each formulation.

Table 11.2 Formulations Prepared for Temozolomide Release.

Formulation	Active ingredient/ Formulation	Mt amount (mg)	HPMC amount (mg)	HPMC ratio (%) (based on total carrier amount)	200 mg/L TMZ solution (mL)
F1	1/10	270	0	0	150
F2	1/10	243	27	10	150
F3	1/10	202.5	67.5	25	150
F4	1/5	120	0	0	150
F5	1/5	108	12	10	150
F6	1/5	90	30	25	150

*Carrier material: Mt + HPMC

11.6 Calibration of Standard Curve of Temozolomide

To determine the concentration of TMZ in solution or after drug release, we performed analyses to identify the wavelengths at which it exhibited significant absorbance levels, utilizing a UV-visible spectrophotometer. Various concentrations of TMZ solutions, spanning from 0 to 50 mg/L, were accurately prepared. Spectra within the wavelength range of 200-400 nm were then recorded using a Shimadzu UV-Vis Mini 1240 UV-visible spectrophotometer. The wavelength at which the drug exhibited the most prominent peak absorbance was determined. Subsequent measurements involved assessing absorbance readings at this specific wavelength.

Figure 11.6 Prepared capsules from each formulations.

11.7 Releasing TMZ from HPMC modified Mt

The release profiles of TMZ from the formulated preparations were evaluated in simulated gastric fluid. This fluid was composed of 2.0 g NaCl, 80 mL 1.0 N HCl, and distilled water adjusted to 420 mL, resulting in a pH of 1.2. Each capsule from every formulation was placed inside a 10 cm dialysis membrane with small pores, which held 5 mL of simulated gastric fluid. These dialysis membranes were positioned in beakers filled with 250 mL of simulated gastric fluid and kept on a magnetic stirrer at 37°C (as shown in Figure 11.7). The collection of samples occurred at different time points, specifically at intervals of 15, 30, 45, 60, 90, 120, 180, 240, 300, and 360 minutes, from each beaker. This was conducted to assess the release of TMZ from the capsules. The analysis was carried out using a UV-visible spectrophotometer at 289 nm, and a standard curve of TMZ was used for this purpose. The entire experiment was performed in a 250 mL volume of simulated gastric fluid, and it's worth noting that 50 mg of the product is believed to contain 5 mg of TMZ, leading to a maximum concentration of 30 mg/L (ppm) representing 100% release. The percentage of TMZ release was calculated using the following formula.

$$\text{TMZ release } \% = \frac{\text{TMZ release at certain time}}{\text{Total loaded TMZ (20 mg)}} \times 100 \qquad (11.1)$$

Figure 11.7 Dialysis membranes positioned in beakers filled with 250 mL of simulated gastric fluid and kept on a magnetic stirrer at 37°C.

12. RESULTS and DISCUSSION

In this section, we have presented the findings from experiments encompassing the characterization of Mt and the release of TMZ from the designed nanocomposite.

12.1 Montmorillonite Characterization

The Mt characterization outcomes indicate that the sedimentation technique employed for Mt beneficiation is remarkably successful in refining and enhancing Mt. In the subsequent sections, we will present and delve into these findings.

12.1.1 XRD and XRF Results

The XRD patterns revealed in Figure 12.1 indicate that the initial clay samples predominantly consisted of montmorillonite (Mt) minerals, with minimal traces of non-clay minerals such as mica, clinoptilolite (zeolite), opal (C-T), quartz, calcite, feldspar, and faint indications of kaolinite. The sedimentation-based beneficiation methods proved highly efficient in eliminating the majority of gangue minerals from the raw Mt (as depicted in Figure 12.1). Consequently, only minor amounts of feldspar, calcite, and opal (C-T) remained in the Mt products post-beneficiation. This discrepancy could be attributed to the presence of particles smaller than 5 micrometers suspended in the water, resembling clay particles, which might have shifted to the beneficiated product's side.

The XRF analysis data provided in Table 12.1 reveal that the samples primarily consist of silicon and aluminum oxide, collectively constituting over 80% of the composition. This composition strongly indicates the presence of clay minerals. Additionally, we computed the $(Na_2O+K_2O)/(CaO+MgO)$ ratio, which was determined to be 0.67. Ratios surpassing 0.33 signify that the Mt samples belong to the intermediate category, indicating their classification as sodium montmorillonite clays, as previously defined by Yüce and Güney (Yüce and Güney, 2014). The significant decline in the calcium ratio within the refined samples suggests the effective extraction of calcite minerals from the

initial samples. More precisely, the decrease in Na2O content post-beneficiation can be linked to the removal of sodium-rich feldspar minerals. These findings align cohesively with the XRD data we have gathered.

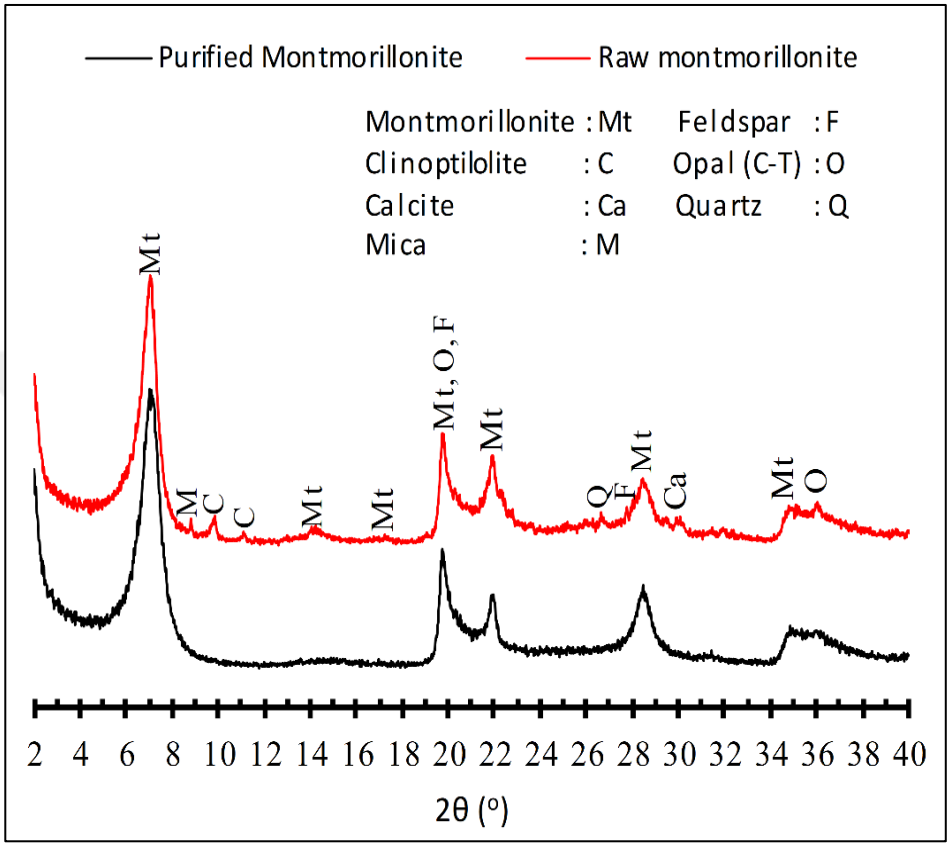

Figure 12.1 XRD patterns of raw and beneficiated clays.

Table 12.1 XRF analysis of raw and purified Mt.

	Quantity (%)	
Component	Mt-Raw	Mt-Sed
SiO_2	62.23	62.19
Al_2O_3	19.06	20.2
Fe_2O_3	3.63	3.99
MgO	2.7	2.93
Na_2O	2.61	2.02
CaO	2.05	0.74
K_2O	0.65	0.44
LOI	6.30	7.0

12.1.2 SEM and TEM Results

When observing Montmorillonite (Mt) clay through an electron microscope, it frequently presents a structure resembling honeycombs, cornflakes, and a leaf-like appearance (Karakaya, 2006, Keller et al., 1986). Scanning Electron Microscope (SEM) images (Figure 12.2-a) indicated that Mt clays consist of particle clusters with smooth surfaces, showcasing a leafy-layered structure with curved edges. Transmission Electron Microscope (TEM) images (Figure 12.2-b) further illustrated a multi-layered arrangement, with successive layers exhibiting parallel and flat surfaces.

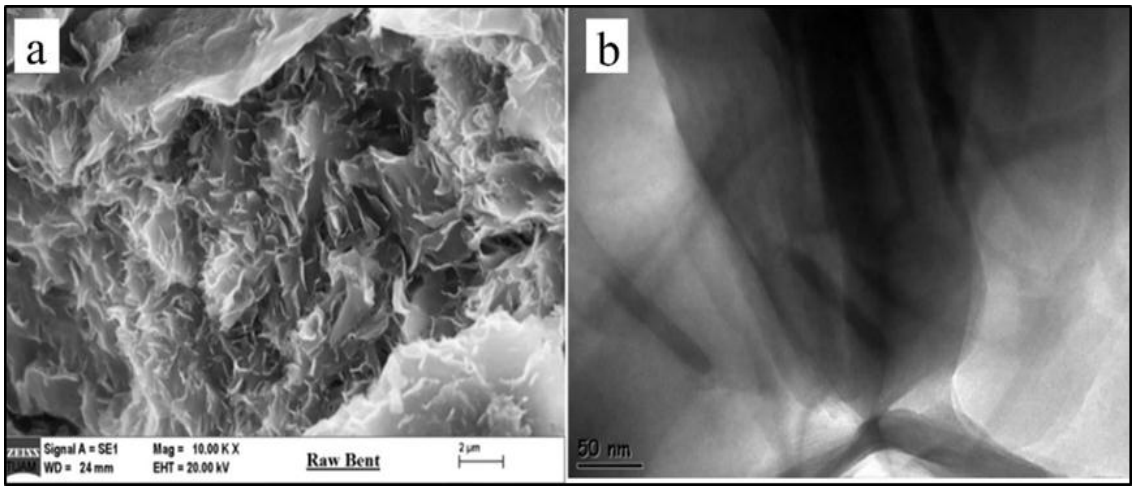

Figure 12.2 (a) Scanning Electron Microscope (SEM) and (b) Transmission Electron Microscope (TEM) images of Montmorillonite clays

12.1.3 SBET Results

The Brunauer-Emmett-Teller (BET) method (Brunauer et al., 1938) was employed to assess the specific surface area (SBET) of Montmorillonite (Mt) using a Micromeritics Gemini 2360 device. Analysis of N2 gas adsorption-desorption data resulted in an SBET value of 89.5 m^2/g for the Mt.

12.1.4 Particle Size Distributions and Zeta Potential Results

The examination of particle size distributions (Figure 12.3) revealed the presence of particles exceeding 10 micrometers in the initial clay samples, making up

approximately 20-25 percent of the volume, likely attributed to gangue minerals. As anticipated, the clay samples subjected to sedimentation beneficiation exhibited more confined size distributions within the range of 0.3-10 micrometers, representing a noteworthy enhancement compared to the raw clay samples. Comparable findings were documented by Shah et al. (Shah et al., 2013a, Shah et al., 2013b), who observed that the particle size distribution of sedimentation-benefited Montmorillonite spanned from 0.3-7.5 micrometers.

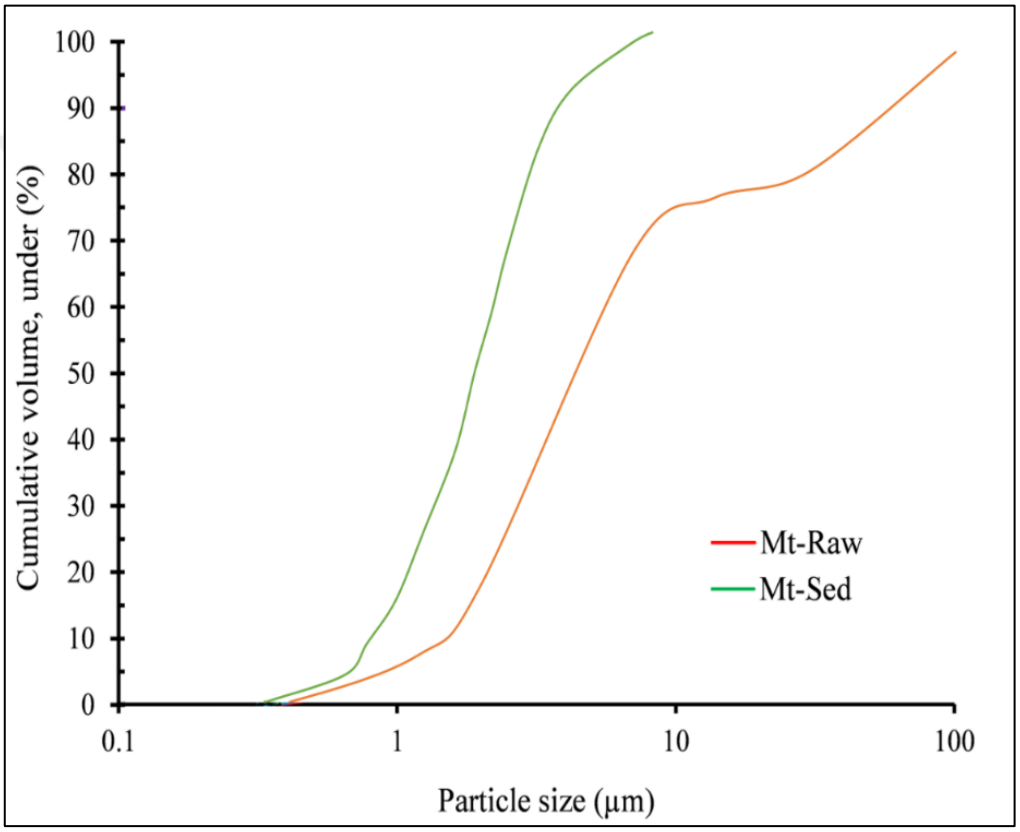

Fiduri 12.3 Particle size distributions of montmorillonite in its natural state and after beneficiation.

Table 12.2 presents the d_{90}, d_{50}, and d_{10} values for both the original and refined clay samples. These values denote the cumulative volumes (90%, 50%, and 10%) of particles smaller than a specified size in the sample. For example, the d_{90} value for the refined Montmorillonite signifies that 90% of the sample comprises particles smaller than 3.82 micrometers. The analysis indicated that the purified clays predominantly consisted of particles below 5 micrometers, aligning with the definition of clay minerals

(Lagaly, 2013). Additionally, both clay samples contained particles as small as approximately 300 nm, indicating the presence of submicron minerals in these clays. As depicted in Figure 12.3 and detailed in Table 12.2, sedimentation-based products exhibited narrower particle size distributions with minimal fluctuations. The data underscored that sedimentation beneficiation methods function by segregating particles based on their size differences. However, it was evident from these parameters that the removal of particles smaller than 5 micrometers through sedimentation techniques presented considerable challenges. Furthermore, the beneficiation yields from the clay beneficiation experiments were determined by calculating the weight ratio of the product obtained after beneficiation to the initially fed product, which amounted to approximately 67.5%.

Table 12.2 Particle size distributions of montmorillonite in its original state and after beneficiation

Clay Samples	d_{10} (μm)	d_{50} (μm)	d_{90} (μm)
Raw Montmorillonite	1.24	3.81	48.79
Beneficiated Montmorillonite	0.85	2.03	3.82

Measurements of Zeta potential (ζ) was executed in 10^-3 M NaCl solutions with ratio of 0.01 wt%. The ζ profiles of Montmorillonite clay are depicted in Figure 12.4, reaffirming its negatively charged surface. It is noteworthy that even in highly acidic conditions, Mt clay sustained a negative surface charge, ascribed to the introduction of hydronium ions amid its clay layers due to a substantial cation exchange capacity. At the lowest pH value (1.91), Montmorillonite clay's ζ value registered -29.2 mV, while at a pH of 11.46, it recorded -41.6 mV. Hence, it can be deduced that the pH exhibited a marginal influence on the ζ of Montmorillonite clay.

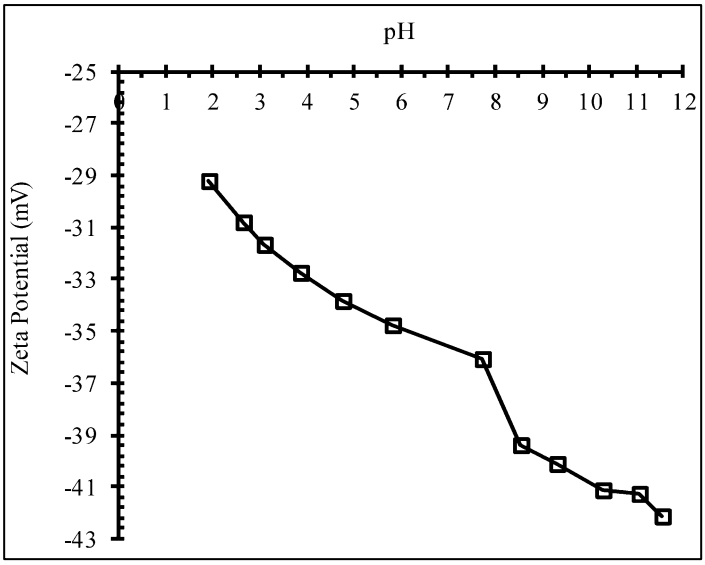

Figure 12.4 Zeta potential profile of montmorillonite.

12.2 TMZ Releasing Results

The outcomes of releasing TMZ loaded onto HPMC-modified Mt revealed that formulation 6, with an HPMC ratio of 25% based on the total carrier amount, exhibited the most effective control over the release of TMZ from Mt carriers.

12.3 Standard Curve of Temozolomide Releasing

The results obtained from the UV spectrophotometer indicate that there is a linear correlation between the concentration of TMZ and its UV absorbance, as illustrated in Figure12.5, particularly at its peak wavelength of 289 nm. 9 different TMZ solutions (0.5, 1.0, 2.0, 4.0, 6.0, 8.0, 10, 20, 50 mg/L) were prepared by dilution from 500 mg/L TMZ stock solution and measurements were performed UV device.

Calibration equation and determination coefficient (r^2) were determined by drawing the calibration curve with the obtained data Therefore, the UV spectrophotometer method proves to be a suitable approach for measuring the concentration of released TMZ.

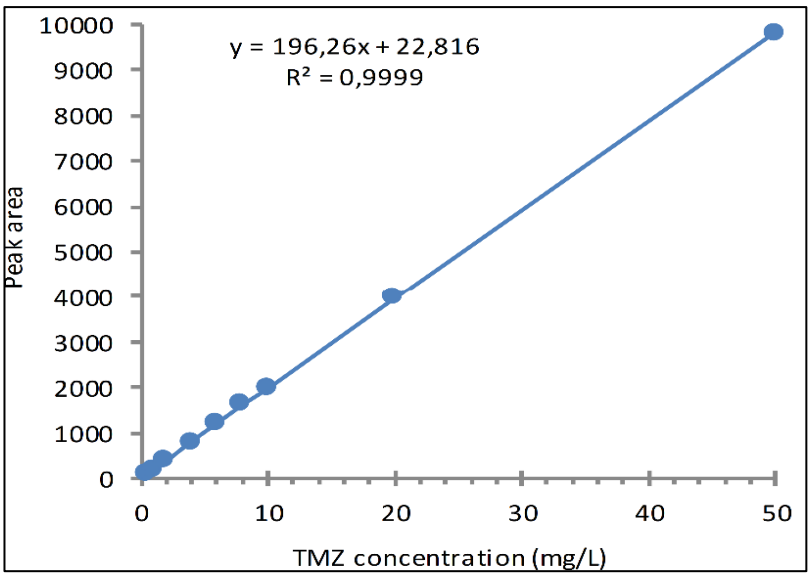

Figure 12.5 The linear relation between TMZ concentration and UV absorbance.

12.4 Releasing TMZ from HPMC Modified Mt

Mauchly's Test of Sphericity revealed a deviation from the sphericity assumption (p-value < 0.05), prompting the utilization of the Greenhouse-Geisser test to address this deviation. This subsequent test confirmed a statistically significant distinction between each formulation at different time points (p-value < 0.001), validating the substantial impact of formulation on TMZ release (p-value < 0.005). Subsequently, a repeated measures test was conducted to examine TMZ release within each formulation, followed by Post Hoc tests to assess TMZ release at distinct time points for each formulation.

The results obtained from the TMZ release study on HPMC-modified Mt unveiled that the formulations 3 and 6, containing 25% HPMC with Mt-HPMC ratios of 1/10 and 1/5, respectively, exhibited superior control over TMZ release during late time points (300-360 minutes) compared to all other formulations, displaying statistically significant differences (p-value < 0.05) (Tables 12.3 and 12.4). Interestingly, formulation 6 demonstrated the best control over TMZ release during early time points (15-240 minutes) among all formulations, also exhibiting significant differences (p-value < 0.05) (Figure 12.6 and Table 12.4). These findings strongly suggest that the combination of 25% HPMC with a 1/5 Mt-HPMC ratio is the most effective for drug loading purposes.

Additionally, formulations 2 and 5, comprising 10% HPMC with Mt-HPMC ratios of 1/10 and 1/5, respectively, showcased better control over TMZ release compared to formulations 1 and 5, which lacked HPMC. These differences were statistically significant (p-value < 0.05) (Figure 12.6 and Tables 12.3 and 12.4). This reaffirms the positive impact of HPMC-modified Mt clays as effective crosslinkers, notably

influencing controlled drug release.

Table 12.3 Formulations Prepared for Temozolomide Release.

Formulation Number	Mt amount (mg)	HPMC amount (mg)	HPMC ratio (%) (based on total carrier amount)	Mean TMZ release (%) after 360 min
1	270	0	0	98.0±0.5
2	243	27	10	97.6±2.2 *
3	202.5	67.5	25	90.8±0.7 **
4	120	0	0	99.0±0.1
5	108	12	10	96.1±1.9 *
6	90	30	25	89.9±0.1 **

* p-value <0.05 in compare with F1 and F4. ** p-value <0.05 in compare with F1 and F4.

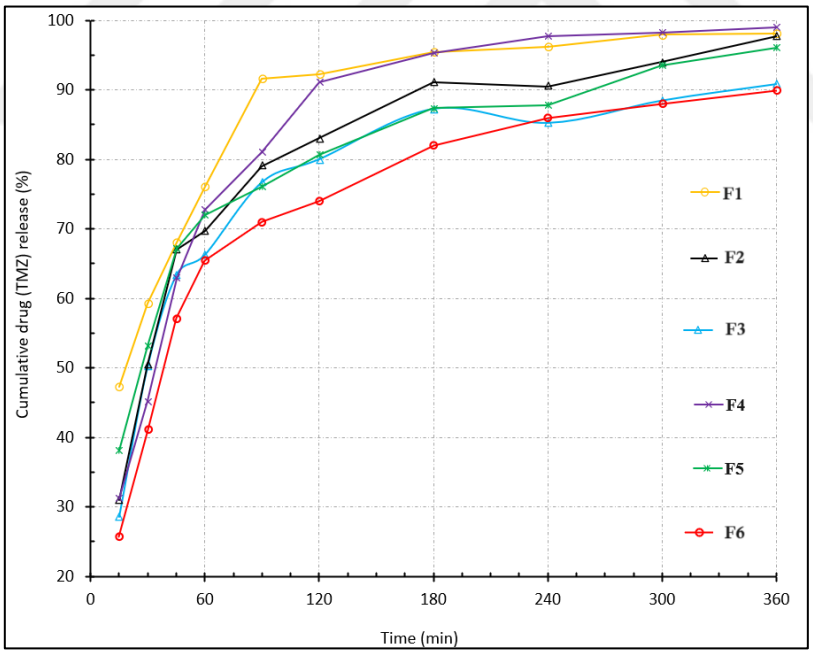

Figure 12.6 TMZ release profiles as a function of time of all formulations.

According to the data obtained from TMZ release profiles, a rapid release started in the first 15 minutes in all drug formulations except F1 and this rapid release continued for 45-60 minutes. Thus, at the end of 60 minutes, approximately 60-70% cumulative TMZ release was achieved. In the F1 formulation, rapid release continued for 90 minutes and

cumulative TMZ release reached approximately 92%. The reason for the faster release in the F1 formulation is that the drug carrier system consists only of Mt clay, that is, there is no HPMC in the formulation. It has thus been proven that HPMC molecules cause delayed release because they cover the surface of TMZ-loaded Mt clay. Again, it was determined that the F4 formulation exhibited a rapid release of TMZ since it did not contain HPMC. It was determined that TMZ release was slower as the HPMC ratio increased in the formulations.

Another result obtained from the release profiles is that the carrier system and TMZ composition ratio change the release kinetics. It was determined that the release was slower in formulations with a TMZ/carrier system ratio of 1/5 compared to those with a 1/10 ratio. This can be explained by the fact that in 1/5 ratio formulations, the TMZ ratio is higher than the carrier system, which causes a higher driving force. Namely, it can be said that as the adsorbate (TMZ) concentration increases, the mass transfer between the clay layers becomes more intense and stronger. Thus, when the TMZ concentration is less than the amount of clay, adsorption mostly occurs on clay surfaces, while as the concentration increases, adsorption occurs on the surface and at the same time, intense adsorption occurs between the clay layers. During the drug release process, TMZ molecules accumulated between clay layers show slower release kinetics than molecules accumulated on the surfaces. According to the release profiles, it was seen that as the HPMC ratio increased, the cumulative TMZ release amount decreased slightly. This situation can be explained by the fact that TMZ molecules accumulated in clay pores are completely covered by HPMC molecules and are trapped in some deep pores and cannot be released.

As a result, it was determined that the F6 formulation showed the best controlled release kinetics. The F6 formulation exhibited rapid TMZ release of 50% levels in the first 45 minutes. In the following period, the release occurred more slowly for 360 minutes and reached approximately 90%.

13. DRUG RELEASE KINETICS

In order to explain the TMZ release kinetics of the obtained formulations, the data obtained from in vitro release studies were evaluated with several different kinetic models. The correlation coefficients (r^2) and "n" values obtained with the kinetic models used are given in Table 13.1.

Table 13.1 In vitro drug release parameters obtained using different kinetic models.

Formulation	Zero order (r^2)	First order (r^2)	Higuchi (r^2)	Hixson-Crowell (r^2)	Korsmeyer-Peppas	
					n	(r^2)
F1	0.8072	0.7534	0.9138	0.7729	0.3437	0.9992
F2	0.7433	0.6198	0.8636	0.6616	0.7762	0.9681
F3	0.7564	0.6264	0.8807	0.6714	0.6213	0.9642
F4	0.8162	0.7088	0.9229	0.7470	0.6237	0.9921
F5	0.8193	0.7372	0.9197	0.7662	0.4314	0.9642
F6	0.7409	0.6187	0.8628	0.6506	0.4692	0.9229

As seen in Table 13.1, TMZ release of the produced formulations can be well modeled with Korsmeyer-Peppas and Hixson kinetics. However, n coefficient values in the Korsmeyer-Peppas model being less than 0.5 are associated with the presence of controlled drug diffusion (Fickian mechanism) and ion exchange mechanism (Chakraborty et al., 2013).

14. CONCLUSION

The examination of unprocessed clay ores revealed that the samples were primarily composed of smectite minerals, primarily Mt, with minor quantities of non-clay minerals (feldspar, quartz, calcite, opal, mica, clinoptilolite). Oriented sample XRD analysis confirmed the dominance of montmorillonite in both clay samples and the absence of other minerals. Semi-quantitative XRD analysis estimated that non-clay minerals constituted 15-20% of the Mt ore. This analysis, in conjunction with XRF data, classified the Mt sample as high-quality sodium clay.

The commercial bentonite ores (Mt) were effectively purified through sedimentation, capitalizing on the particle size disparity between clay (Mt) and non-clay minerals. When clays were soaked in water for an adequate duration, they dispersed completely, eliminating the need for prolonged mechanical dispersion before beneficiation studies. In sedimentation beneficiation tests at a 1.0 wt.% solid ratio, it was established that an 8-hour period was ample for the sedimentation of particles exceeding 2 μm. These results confirmed that the purified Mt clay possessed a purity level exceeding 90%. Sedimentation yielded a 67.5% purity for Mt clay. Consequently, for nanocomposite product preparation, the Mt clay produced at a higher purity level was deemed suitable.

In the TMZ release study using HPMC-modified Mt, formulations containing 25% HPMC with Mt-HPMC ratios of 1/10 and 1/5 (formulations 3 and 6) showed superior control over TMZ release in late time points compared to other formulations. Specifically, formulation 6 exhibited the best control over early TMZ release. Additionally, formulations with 10% HPMC and varying Mt-HPMC ratios demonstrated better control over TMZ release compared to formulations without HPMC. These findings highlight the effectiveness of HPMC-modified Mt clays as crosslinkers, influencing controlled drug release.

These results underscore the favorable impact of HPMC-modified Mt on the controlled release of TMZ. This research introduces an innovative method for controlled drug release, leveraging the distinctive qualities of Mt clay and HPMC. It offers potential

solutions to the challenges posed by TMZ and opens up promising avenues for treating cancers. The study serves as a foundational step for further exploration and the advancement of improved treatment strategies for GBM patients.

15. REFERENCES

Aboudi Mana, S. C., Hanafiah, M. M. & Chowdhury, A. J. K. 2017. Environmental characteristics of clay and clay-based minerals. GeoloGy, ecoloGy, and landscapes, 1**,** 155-161.

Ahad, A., Shakeel, F., Raish, M., Ahmad, A., Bin Jardan, Y. A., Al-Jenoobi, F. I. & Al-Mohizea, A. M. 2022. Thermodynamic Solubility Profile of Temozolomide in Different Commonly Used Pharmaceutical Solvents. Molecules, 27.

Ahmed, B., Qadir, M. I. & Ghafoor, S. 2020. Malignant Melanoma: Skin Cancer-Diagnosis, Prevention, and Treatment. Crit Rev Eukaryot Gene Expr, 30**,** 291-297.

Akhtar, U., Hossain, M., Miran, M. & Mollah, M. 2014. Synthesis and characterization of porous silica and polyaniline-porous silica composite materials with high surface area. Bangladesh Journal of Scientific and Industrial Research, 49**,** 1-8.

Aldape, K., Brindle, K. M., Chesler, L., Chopra, R., Gajjar, A., Gilbert, M. R., Gottardo, N., Gutmann, D. H., Hargrave, D., Holland, E. C., Jones, D. T. W., Joyce, J. A., Kearns, P., Kieran, M. W., Mellinghoff, I. K., Merchant, M., Pfister, S. M., Pollard, S. M., Ramaswamy, V., Rich, J. N., Robinson, G. W., Rowitch, D. H., Sampson, J. H., Taylor, M. D., Workman, P. & Gilbertson, R. J. 2019. Challenges to curing primary brain tumours. Nat Rev Clin Oncol, 16**,** 509-520.

Ammala, A. 2013. Biodegradable polymers as encapsulation materials for cosmetics and personal care markets. International journal of cosmetic science, 35**,** 113-124.

Anirudhan, T., Gopal, S. S. & Sandeep, S. 2014. Synthesis and characterization of montmorillonite/N-(carboxyacyl) chitosan coated magnetic particle nanocomposites for controlled delivery of paracetamol. Applied clay science, 88**,** 151-158.

Arakawa, Y., Sasaki, K., Mineharu, Y., Uto, M., Mizowaki, T., Mizusawa, J., Sekino, Y., Ono, T., Aoyama, H. & Satomi, K. 2021. A randomized phase III study of short-course radiotherapy combined with Temozolomide in elderly patients with

newly diagnosed glioblastoma; Japan clinical oncology group study JCOG1910 (AgedGlio-PIII). BMC cancer, 21**,** 1-8.

Arora, A. & Somasundaram, K. 2019. Glioblastoma vs temozolomide: can the red queen race be won? Cancer Biol Ther, 20**,** 1083-1090.

Asamoah, R., Nyankson, E., Annan, E., Agyei-Tuffour, B., Efavi, J., Kan-Dapaah, K., Apalangya, V., Damoah, L., Dodoo-Arhin, D. & Tiburu, E. 2018. Industrial applications of clay materials from ghana-a review. Oriental Journal of Chemistry, 34**,** 1719.

Baek, M., Lee, J.-A. & Choi, S.-J. 2012. Toxicological effects of a cationic clay, montmorillonite in vitro and in vivo. Molecular & Cellular Toxicology, 8**,** 95-101.

Barrié, M., Couprie, C., Dufour, H., Figarella-Branger, D., Muracciole, X., Hoang-Xuan, K., Braguer, D., Martin, P. M., Peragut, J. C., Grisoli, F. & Chinot, O. 2005. Temozolomide in combination with BCNU before and after radiotherapy in patients with inoperable newly diagnosed glioblastoma multiforme. Annals of Oncology, 16**,** 1177-1184.

Bergaya, F. & Lagaly, G. 2006. General introduction: clays, clay minerals, and clay science. Developments in clay science, 1**,** 1-18.

Bergaya, F. & Lagaly, G. 2013. Handbook of clay science, Newnes.

Boogerd, W., De Gast, G. C. & Dalesio, O. 2007. Temozolomide in advanced malignant melanoma with small brain metastases: can we withhold cranial irradiation? Cancer, 109**,** 306-312.

Boylu, F., Hojiyev, R., Ersever, G., Ulcay, Y. & Çelik, M. 2012. Production of ultrapure bentonite clays through centrifugation techniques. Separation Science and Technology, 47**,** 842-849.

Brenner, A. V., Linet, M. S., Fine, H. A., Shapiro, W. R., Selker, R. G., Black, P. M. & Inskip, P. D. 2002. History of allergies and autoimmune diseases and risk of brain tumors in adults. Int J Cancer, 99**,** 252-9.

Brown, G. T. & Brindley, G. 1980. X-ray diffraction procedures for clay mineral

identification.

Brunauer, S., Emmett, P. H. & Teller, E. 1938. Adsorption of gases in multimolecular layers. Journal of the American chemical society, 60**,** 309-319.

Bush, N. a. O., Hervey-Jumper, S. L. & Berger, M. S. 2019. Management of glioblastoma, present and future. World neurosurgery, 131**,** 328-338.

Carretero, M., Gomes, C. & Tateo, F. 2013. Clays, drugs, and human health. Developments in clay science. Elsevier.

Carretero, M. I. 2002. Clay minerals and their beneficial effects upon human health. A review. Applied Clay Science, 21**,** 155-163.

Carretero, M. I. & Pozo, M. 2009. Clay and non-clay minerals in the pharmaceutical industry: Part I. Excipients and medical applications. Applied Clay Science, 46**,** 73-80.

Carretero, M. I. & Pozo, M. 2010. Clay and non-clay minerals in the pharmaceutical and cosmetic industries Part II. Active ingredients. Applied Clay Science, 47**,** 171-181.

Chakraborty, J., Roychowdhury, S., Sengupta, S. and Ghosh, S. (2013). Mg-Al layered double hydroxide-methotrexate nanohybrid drug delivery system: evaluation of efficacy. *Materials Scence and Engineering C*, 33: 2168-2174.

Choy, J.-H., Choi, S.-J., Oh, J.-M. & Park, T. 2007. Clay minerals and layered double hydroxides for novel biological applications. Applied Clay Science, 36**,** 122-132.

Ciftci, H. 2021. An introduction to montmorillonite purification. Montmorillonite Clay. IntechOpen.

Çiftçi, H., Arpa, M. D., Gülaçar, İ. M., Özcan, L. & Ersoy, B. 2020a. Development and evaluation of mesoporous montmorillonite/magnetite nanocomposites loaded with 5-Fluorouracil. Microporous and Mesoporous Materials, 303**,** 110253.

Çiftçi, H., Ersoy, B. & Evcin, A. 2020b. Purification of Turkish bentonites and investigation of the contact angle, surface free energy and zeta potential profiles of organo-bentonites as a function of CTAB concentration. Clays and Clay

Minerals, 68**,** 250-261.

Collins, I. & Workman, P. 2006. New approaches to molecular cancer therapeutics. Nat Chem Biol, 2**,** 689-700.

Dziadziuszko, R., Ardizzoni, A., Postmus, P., Smit, E., Price, A., Debruyne, C., Legrand, C., Giaccone, G. & Group, E. L. C. 2003. Temozolomide in patients with advanced non-small cell lung cancer with and without brain metastases: a phase II study of the EORTC Lung Cancer Group (08965). European Journal of Cancer, 39**,** 1271-1276.

Eskanlou, A. & Huang, Q. 2021. Phosphatic waste clay: Origin, composition, physicochemical properties, challenges, values and possible remedies–A review. Minerals Engineering, 162**,** 106745.

Friuli, V., Pisani, S., Conti, B., Bruni, G. & Maggi, L. 2022. Tablet formulations of polymeric electrospun fibers for the controlled release of drugs with pH-dependent solubility. Polymers, 14**,** 2127.

Fu, W, Hua, L. & Zhang, W. 2017. Experimental and modeling assessment of the roles of hydrophobicity and zeta potential in chemically modified poly (ether sulfone) membrane fouling kinetics. Industrial & Engineering Chemistry Research, 56**,** 8580-8589.

Hassen, J. H., Abdalkadir, H. K. & Abed, S. F. 2023. An overview of medical applications of montmorillonite clay. Journal of Medical Science, 92**,** e826-e826.

Heller-Kallai, L. 2013. Thermally modified clay minerals. Developments in clay science. Elsevier.

Hochberg, F., Toniolo, P., Cole, P. & Salcman, M. 1990. Nonoccupational risk indicators of glioblastoma in adults. J Neurooncol, 8**,** 55-60.

Hodges, L. C., Smith, J. L., Garrett, A. & Tate, S. 1992. Prevalence of glioblastoma multiforme in subjects with prior therapeutic radiation. J Neurosci Nurs, 24**,** 79-83.

Hojiyev, R., Ersever, G., Karaağaçlıoğlu, İ. E., Karakaş, F. & Boylu, F. 2016. Changes

on montmorillonite characteristics through modification. Applied clay science, 127**,** 105-110.

Hojiyev, R., Ulcay, Y. & Çelik, M. S. 2017. Development of a clay-polymer compatibility approach for nanocomposite applications. Applied Clay Science, 146**,** 548-556.

Huang, W.-C., Hu, S.-H., Liu, K.-H., Chen, S.-Y. & Liu, D.-M. 2009. A flexible drug delivery chip for the magnetically-controlled release of anti-epileptic drugs. Journal of Controlled Release, 139**,** 221-228.

Ibrahim, M. A. & Abdellatif, A. A. 2021. Applications of nanopharmaceuticals in delivery and targeting. Nanopharmaceuticals: Principles and Applications Vol. 1**,** 73-114.

Iliescu, R. I., Andronescu, E., Ghitulica, C. D., Voicu, G., Ficai, A. & Hoteteu, M. 2014. Montmorillonite–alginate nanocomposite as a drug delivery system – incorporation and in vitro release of irinotecan. International Journal of Pharmaceutics, 463**,** 184-192.

Im, G. J., Chae, S. Y., Lee, K. C. & Lee, D. S. 2009. Controlled release of insulin from pH/temperature-sensitive injectable pentablock copolymer hydrogel. Journal of Controlled Release, 137**,** 20-24.

Irannajad, M., Nuri, O. S. & Mehdilo, A. 2019. Surface dissolution-assisted mineral flotation: A review. Journal of Environmental Chemical Engineering, 7**,** 103050.

Ismadji, S., Soetaredjo, F. E., Ayucitra, A., Ismadji, S., Soetaredjo, F. E. & Ayucitra, A. 2015. Modification of clay minerals for adsorption purpose. Clay Materials for Environmental Remediation**,** 39-56.

Iturrioz-Rodríguez, N., Sampron, N. & Matheu, A. 2023. Current advances in temozolomide encapsulation for the enhancement of glioblastoma treatment. Theranostics, 13**,** 2734.

Iversen, T. Z. 2013. Immune modulations during chemoimmunotherapy & novel vaccine strategies—in metastatic melanoma and non small-cell lung cancer. Dan Med J, 60**,** B4774.

Jain, S. & Datta, M. 2015. Oral extended release of dexamethasone: Montmorillonite–PLGA nanocomposites as a delivery vehicle. Applied Clay Science, 104**,** 182-188.

Jatyan, R., Sahel, D. K., Singh, P., Sakhuja, R., Mittal, A. & Chitkara, D. 2023. Temozolomide-fatty acid conjugates for glioblastoma multiforme: In vitro and in vivo evaluation. Journal of Controlled Release, 359**,** 161-174.

Jayrajsinh, S., Shankar, G., Agrawal, Y. K. & Bakre, L. 2017. Montmorillonite nanoclay as a multifaceted drug-delivery carrier: A review. Journal of Drug Delivery Science and Technology, 39**,** 200-209.

Joshi, G. V., Kevadiya, B. D., Patel, H. A., Bajaj, H. C. & Jasra, R. V. 2009. Montmorillonite as a drug delivery system: intercalation and in vitro release of timolol maleate. International Journal of Pharmaceutics, 374**,** 53-57.

Joshi, S. C. 2011. Sol-gel behavior of hydroxypropyl methylcellulose (HPMC) in ionic media including drug release. Materials, 4**,** 1861-1905.

Karakaya, M. Ç. 2006. Kil minerallerinin özellikleri ve tanımlama yöntemleri, ODTÜ.

Keller, W., Reynolds, R. & Inoue, A. 1986. Morphology of clay minerals in the smectite-to-illite conversion series by scanning electron microscopy. Clays and Clay Minerals, 34**,** 187-197.

Kevadiya, B. D., Patel, T. A., Jhala, D. D., Thumbar, R. P., Brahmbhatt, H., Pandya, M. P., Rajkumar, S., Jena, P. K., Joshi, G. V. & Gadhia, P. K. 2012. Layered inorganic nanocomposites: a promising carrier for 5-fluorouracil (5-FU). European Journal of Pharmaceutics and Biopharmaceutics, 81**,** 91-101.

Khater, E.-S., Bahnasawy, A., Gabal, B. A., Abbas, W. & Morsy, O. 2023. Effect of adding nano-materials on the properties of hydroxypropyl methylcellulose (HPMC) edible films. Scientific Reports, 13**,** 5063.

Kleihues, P. & Ohgaki, H. 2000. Phenotype vs genotype in the evolution of astrocytic brain tumors. Toxicol Pathol, 28**,** 164-70.

Kryuchkova, M., Batasheva, S., Akhatova, F., Babaev, V., Buzyurova, D., Vikulina, A., Volodkin, D., Fakhrullin, R. & Rozhina, E. 2021. Pharmaceuticals removal by adsorption with montmorillonite nanoclay. International Journal of Molecular

Sciences, 22**,** 9670.

Krzak, A. & Bilewicz, R. 2020. Voltammetric/UV–Vis study of temozolomide inclusion complexes with cyclodextrin derivatives. Bioelectrochemistry, 136**,** 107587.

Kumar, A. & Lingfa, P. 2020. Acid-activated sodium bentonite and kaolin clay: Comparative study by physicochemical properties. Combinatorial Chemistry & High Throughput Screening, 23**,** 433-445.

Lagaly, G. 2013. Colloid Clay Science In: BERGAYA, F.; THENG, BKG; LAGALY, G.(Eds.), Handbook of Clay Science. Elsevier.

Lal, S. & Datta, M. 2015. In vitro prolonged gastric residence and sustained release of atenolol using novel clay polymer nanocomposite. Applied Clay Science, 114**,** 412-421.

Langer, R. & Peppas, N. 1983. Chemical and physical structure of polymers as carriers for controlled release of bioactive agents: a review. Journal of Macromolecular Science-Reviews in Macromolecular Chemistry and Physics, 23**,** 61-126.

Lee, Y.-H., Kuo, T.-F., Chen, B.-Y., Feng, Y.-K., Wen, Y.-R., Lin, W.-C. & Lin, F. 2005. Toxicity assessment of montmorillonite as a drug carrier for pharmaceutical applications: yeast and rats model. Biomedical Engineering: Applications, Basis and Communications, 17**,** 72-78.

Li, H, Chen, C., An, Q., Huo, G. & Run, M. 2018a. Photo-responsive nanoparticles for β-lapachone delivery in vitro. Chinese Chemical Letters, 29**,** 1347-1349.

Li, J., Tian, S., Tao, Q., Zhao, Y., Gui, R., Yang, F., Zang, L., Chen, Y., Ping, Q. & Hou, D. 2018b. Montmorillonite/chitosan nanoparticles as a novel controlled-release topical ophthalmic delivery system for the treatment of glaucoma. International journal of nanomedicine**,** 3975-3987.

Liang, L., Xi, F., Tan, W., Meng, X., Hu, B. & Wang, X. 2021. Review of organic and inorganic pollutants removal by biochar and biochar-based composites. Biochar, 3**,** 255-281.

Lin, L., Cai, J., Tan, Z., Meng, X., Li, R., Li, Y. & Jiang, C. 2021. Mutant IDH1

Enhances Temozolomide Sensitivity via Regulation of the ATM/CHK2 Pathway in Glioma. Cancer Res Treat, 53**,** 367-377.

Linkous, A. G. & Yazlovitskaya, E. M. 2011. Angiogenesis in glioblastoma multiforme: navigating the maze. Anticancer Agents Med Chem, 11**,** 712-8.

Lipinski, C. & Hopkins, A. 2004. Navigating chemical space for biology and medicine. Nature, 432**,** 855-61.

Louis, D. N., Perry, A., Wesseling, P., Brat, D. J., Cree, I. A., Figarella-Branger, D., Hawkins, C., Ng, H., Pfister, S. M. & Reifenberger, G. 2021. The 2021 WHO classification of tumors of the central nervous system: a summary. Neuro-oncology, 23**,** 1231-1251.

Mandracchia, D. & Tripodo, G. 2020. Micro and nano-drug delivery systems.

Marchuk, S. 2016. The Dynamics of Potassium in some Australian soils.

Mašková, E., Kubová, K., Raimi-Abraham, B. T., Vllasaliu, D., Vohlídalová, E., Turánek, J. & Mašek, J. 2020. Hypromellose–A traditional pharmaceutical excipient with modern applications in oral and oromucosal drug delivery. Journal of controlled release, 324**,** 695-727.

Mokhtar, A., Ahmed, A. B., Asli, B., Boukoussa, B., Hachemaoui, M., Sassi, M. & Abboud, M. 2023. Recent Advances in Antibacterial Metallic Species Supported on Montmorillonite Clay Mineral: A Review. Minerals, 13**,** 1268.

Molenaar, R. J., Maciejewski, J. P., Wilmink, J. W. & Van Noorden, C. J. F. 2018. Wild-type and mutated IDH1/2 enzymes and therapy responses. Oncogene, 37**,** 1949-1960.

Molina, J. R., Yang, P., Cassivi, S. D., Schild, S. E. & Adjei, A. A. 2008. Non-small cell lung cancer: epidemiology, risk factors, treatment, and survivorship. Mayo Clin Proc, 83**,** 584-94.

Naeli, M. H., Milani, J. M., Farmani, J. & Zargaraan, A. 2020. Development of innovative ethyl cellulose-hydroxypropyl methylcellulose biopolymer oleogels as low saturation fat replacers: Physical, rheological and microstructural characteristics. International journal of biological macromolecules, 156**,** 792-

804.

Newlands, E. S., Stevens, M. F., Wedge, S. R., Wheelhouse, R. T. & Brock, C. 1997. Temozolomide: a review of its discovery, chemical properties, pre-clinical development and clinical trials. Cancer Treat Rev, 23**,** 35-61.

Nieto, S., Toro, N., Robles, P., Gálvez, E., Gallegos, S. & Jeldres, R. I. 2022. Flocculation of Clay-Based Tailings: Differences of Kaolin and Sodium Montmorillonite in Salt Medium. Materials, 15**,** 1156.

Novak, S. D., Šporar, E., Baumgartner, S. & Vrečer, F. 2012. Characterization of physicochemical properties of hydroxypropyl methylcellulose (HPMC) type 2208 and their influence on prolonged drug release from matrix tablets. Journal of pharmaceutical and biomedical analysis, 66**,** 136-143.

Ohgaki, H., Dessen, P., Jourde, B., Horstmann, S., Nishikawa, T., Di Patre, P. L., Burkhard, C., Schüler, D., Probst-Hensch, N. M., Maiorka, P. C., Baeza, N., Pisani, P., Yonekawa, Y., Yasargil, M. G., Lütolf, U. M. & Kleihues, P. 2004. Genetic pathways to glioblastoma: a population-based study. Cancer Res, 64**,** 6892-9.

Olar, A. & Aldape, K. D. 2014. Using the molecular classification of glioblastoma to inform personalized treatment. J Pathol, 232**,** 165-77.

Oliveira, H., Pérez-Andrés, E., Thevenot, J., Sandre, O., Berra, E. & Lecommandoux, S. 2013. Magnetic field triggered drug release from polymersomes for cancer therapeutics. Journal of Controlled Release, 169**,** 165-170.

Ombaka, O. 2016. Characterization and classification of clay minerals for potential applications in Rugi Ward, Kenya. African Journal of environmental science and Technology, 10**,** 415-431.

Orucoglu, E. & Haciyakupoglu, S. 2015. Bentonite modification with hexadecylpyridinium and aluminum polyoxy cations and its effectiveness in Se (IV) removal. Journal of Environmental Management, 160**,** 30-38.

Ostrom, Q. T., Gittleman, H., Farah, P., Ondracek, A., Chen, Y., Wolinsky, Y., Stroup, N. E., Kruchko, C. & Barnholtz-Sloan, J. S. 2013. CBTRUS statistical report: Primary brain and central nervous system tumors diagnosed in the United States

in 2006-2010. Neuro Oncol, 15 Suppl 2**,** ii1-56.

Ostrom, Q. T., Gittleman, H., Xu, J., Kromer, C., Wolinsky, Y., Kruchko, C. & Barnholtz-Sloan, J. S. 2016. CBTRUS Statistical Report: Primary Brain and Other Central Nervous System Tumors Diagnosed in the United States in 2009-2013. Neuro Oncol, 18**,** v1-v75.

Otunola, B. O. & Ololade, O. O. 2020. A review on the application of clay minerals as heavy metal adsorbents for remediation purposes. Environmental Technology & Innovation, 18**,** 100692.

Ozdemir, O. & Çelik, M. S. 2010. Surface properties and flotation characteristics of boron minerals. The Open Mineral Processing Journal, 3.

Park, J.-H., Shin, H.-J., Kim, M. H., Kim, J.-S., Kang, N., Lee, J.-Y., Kim, K.-T., Lee, J. I. & Kim, D.-D. 2016. Application of montmorillonite in bentonite as a pharmaceutical excipient in drug delivery systems. Journal of Pharmaceutical Investigation, 46**,** 363-375.

Pires, J. 2014. Nanoporous materials: pillared clays and regular silicas as an example of synthesis and their porosity characterization by X-ray diffraction. Química Nova, 37**,** 168-170.

Quirbt, I., Verma, S., Petrella, T., Bak, K. & Charette, M. 2007. Temozolomide for the treatment of metastatic melanoma. Current Oncology, 14**,** 27-33.

Raizer, J. J., Malkin, M. G., Kleber, M. & Abrey, L. E. 2004. Phase 1 study of 28-day, low-dose temozolomide and BCNU in the treatment of malignant gliomas after radiation therapy. Neuro Oncol, 6**,** 247-52.

Rajkumar, S., Kevadiya, B. D. & Bajaj, H. C. 2015. Montmorillonite/Poly (L-Lactide) microcomposite spheres as reservoirs of antidepressant drugs and their controlled release property. asian journal of pharmaceutical sciences, 10**,** 452-458.

Rodríguez-Garnica, P., Salazar-Hernández, M. M., Maldonado-Estudillo, J., Saldaña-Piña, N., Sotelo-Rodríguez, G., Huichapa-Rocha, B., González-García, G., Alatorre-Ordaz, A. & Gutiérrez, J. A. 2019. Nonordered porous silica-based pure inorganic and hybrid organic-inorganic materials prepared by a

nonaqueous, nonthermal sol-gel process. Materials Chemistry and Physics, 229**,** 156-166.

Safdar, R., Omar, A. A., Arunagiri, A., Regupathi, I. & Thanabalan, M. 2019. Potential of Chitosan and its derivatives for controlled drug release applications–A review. Journal of drug delivery science and technology, 49**,** 642-659.

Salcedo, I., Aguzzi, C., Sandri, G., Bonferoni, M. C., Mori, M., Cerezo, P., Sánchez, R., Viseras, C. & Caramella, C. 2012. In vitro biocompatibility and mucoadhesion of montmorillonite chitosan nanocomposite: A new drug delivery. Applied clay science, 55**,** 131-137.

Sanchez-Martin, M., Rodriguez-Cruz, M., Andrades, M. & Sanchez-Camazano, M. 2006. Efficiency of different clay minerals modified with a cationic surfactant in the adsorption of pesticides: influence of clay type and pesticide hydrophobicity. Applied Clay Science, 31**,** 216-228.

Scheurer, M. E., Amirian, E. S., Davlin, S. L., Rice, T., Wrensch, M. & Bondy, M. L. 2011. Effects of antihistamine and anti-inflammatory medication use on risk of specific glioma histologies. Int J Cancer, 129**,** 2290-6.

Shah, L. A., Da Silva Valenzuela, M. D. G., Ehsan, A. M., Díaz, F. R. V. & Khattak, N. S. 2013a. Characterization of Pakistani purified bentonite suitable for possible pharmaceutical application. Applied Clay Science, 83**,** 50-55.

Shah, L. A., Khattak, N., Valenzuela, M., Manan, A. & Díaz, F. V. 2013b. Preparation and characterization of purified Na-activated bentonite from Karak (Pakistan) for pharmaceutical use. Clay Minerals, 48**,** 595-603.

Singla, P., Mehta, R. & Upadhyay, S. N. 2012. Clay modification by the use of organic cations. Green and sustainable chemistry, 2**,** 21-25.

Smolarz, B., Nowak, A. Z. & Romanowicz, H. 2022. Breast Cancer-Epidemiology, Classification, Pathogenesis and Treatment (Review of Literature). Cancers (Basel), 14.

Sondi, I., Milat, O. & Pravdić, V. 1997. Electrokinetic potentials of clay surfaces modified by polymers. Journal of Colloid and Interface Science, 189**,** 66-73.

Stevens, M. F. & Newlands, E. S. 1993. From triazines and triazenes to temozolomide. Eur J Cancer, 29a**,** 1045-7.

Stoyanov, G. S., Dzhenkov, D., Ghenev, P., Iliev, B., Enchev, Y. & Tonchev, A. B. 2018. Cell biology of glioblastoma multiforme: from basic science to diagnosis and treatment. Med Oncol, 35**,** 27.

Stupp, R., Hegi, M. E., Mason, W. P., Van Den Bent, M. J., Taphoorn, M. J., Janzer, R. C., Ludwin, S. K., Allgeier, A., Fisher, B. & Belanger, K. 2009. Effects of radiotherapy with concomitant and adjuvant temozolomide versus radiotherapy alone on survival in glioblastoma in a randomised phase III study: 5-year analysis of the EORTC-NCIC trial. The lancet oncology, 10**,** 459-466.

Sun, X. & Turcan, S. 2021. From Laboratory Studies to Clinical Trials: Temozolomide Use in IDH-Mutant Gliomas. Cells, 10.

Thakkar, J. P., Dolecek, T. A., Horbinski, C., Ostrom, Q. T., Lightner, D. D., Barnholtz-Sloan, J. S. & Villano, J. L. 2014. Epidemiologic and molecular prognostic review of glioblastoma. Cancer Epidemiol Biomarkers Prev, 23**,** 1985-96.

Tiwari, R. 2016. Controlled release drug formulation in pharmaceuticals: a study on their application and properties. World J Pharm Res, 5**,** 1740-1720.

Torrisi, F., Alberghina, C., D'aprile, S., Pavone, A. M., Longhitano, L., Giallongo, S., Tibullo, D., Di Rosa, M., Zappalà, A. & Cammarata, F. P. 2022. The hallmarks of glioblastoma: Heterogeneity, intercellular crosstalk and molecular signature of invasiveness and progression. Biomedicines, 10**,** 806.

Trudeau, M., Crump, M., Charpentier, D., Yelle, L., Bordeleau, L., Matthews, S. & Eisenhauer, E. 2006. Temozolomide in metastatic breast cancer (MBC): a phase II trial of the National Cancer Institute of Canada–Clinical Trials Group (NCIC-CTG). Annals of oncology, 17**,** 952-956.

Uddin, F. 2018. Montmorillonite: An introduction to properties and utilization, IntechOpen London, UK.

Ünal, Ç., Azizy, A., Karabulut, S., Taştekin, D., Akyıldız, A., Yaşar, S., Yalçın, Ş., Çoban, E., Evrensel, T. & Kalkan, Z. 2023. Efficacy of Capecitabine and Temozolomide Regimen in Neuroendocrine Tumors: Data From the Turkish

Oncology Group. The oncologist, 28**,** 875-884.

Urbańska, K., Sokołowska, J., Szmidt, M. & Sysa, P. 2014. Glioblastoma multiforme - an overview. Contemp Oncol (Pozn), 18**,** 307-12.

Vejan, P., Khadiran, T., Abdullah, R. & Ahmad, N. 2021. Controlled release fertilizer: A review on developments, applications and potential in agriculture. Journal of Controlled Release, 339**,** 321-334.

Viseras, C., Cerezo, P., Sanchez, R., Salcedo, I. & Aguzzi, C. 2010. Current challenges in clay minerals for drug delivery. Applied Clay Science, 48**,** 291-295.

Waghule, T., Swetha, K. L., Roy, A., Saha, R. N. & Singhvi, G. 2023. Exploring temozolomide encapsulated PEGylated liposomes and lyotropic liquid crystals for effective treatment of glioblastoma: in-vitro, cell line, and pharmacokinetic studies. European Journal of Pharmaceutics and Biopharmaceutics, 186**,** 18-29.

Wang, R., Peng, Y., Zhou, M. & Shou, D. 2016. Smart montmorillonite-polypyrrole scaffolds for electro-responsive drug release. Applied Clay Science, 134**,** 50-54.

Watson, J. D. & Crick, F. H. 1953. Molecular structure of nucleic acids; a structure for deoxyribose nucleic acid. Nature, 171**,** 737-8.

Wen, H. & Park, K. 2010. Introduction and overview of oral controlled release formulation design. Oral controlled release formulation design and drug delivery: theory to practice**,** 1-19.

Wrensch, M., Jenkins, R. B., Chang, J. S., Yeh, R. F., Xiao, Y., Decker, P. A., Ballman, K. V., Berger, M., Buckner, J. C., Chang, S., Giannini, C., Halder, C., Kollmeyer, T. M., Kosel, M. L., Lachance, D. H., Mccoy, L., O'neill, B. P., Patoka, J., Pico, A. R., Prados, M., Quesenberry, C., Rice, T., Rynearson, A. L., Smirnov, I., Tihan, T., Wiemels, J., Yang, P. & Wiencke, J. K. 2009. Variants in the CDKN2B and RTEL1 regions are associated with high-grade glioma susceptibility. Nat Genet, 41**,** 905-8.

Wu, S., Huang, X. & Du, X. 2015. pH-and redox-triggered synergistic controlled release of a ZnO-gated hollow mesoporous silica drug delivery system. Journal of Materials Chemistry B, 3**,** 1426-1432.

Xi, Y., Mallavarapu, M. & Naidu, R. 2010. Preparation, characterization of surfactants modified clay minerals and nitrate adsorption. Applied Clay Science, 48**,** 92-96.

Yamamuro, S., Takahashi, M., Satomi, K., Sasaki, N., Kobayashi, T., Uchida, E., Kawauchi, D., Nakano, T., Fujii, T., Narita, Y., Kondo, A., Wada, K., Yoshino, A., Ichimura, K. & Tomiyama, A. 2021. Lomustine and nimustine exert efficient antitumor effects against glioblastoma models with acquired temozolomide resistance. Cancer Sci, 112**,** 4736-4747.

Yang, J.-H., Lee, J.-H., Ryu, H.-J., Elzatahry, A. A., Alothman, Z. A. & Choy, J.-H. 2016. Drug–clay nanohybrids as sustained delivery systems. Applied Clay Science, 130**,** 20-32.

Yang, Y.-J., Tao, X., Hou, Q., Ma, Y., Chen, X.-L. & Chen, J.-F. 2010. Mesoporous silica nanotubes coated with multilayered polyelectrolytes for pH-controlled drug release. Acta Biomaterialia, 6**,** 3092-3100.

Yeşilyurt, Z., Boylu, F., Cinku, K., Esenli, F. & Çelik, M. 2014. Simultaneous purification and modification process for organobentonite production. Applied clay science, 95**,** 176-181.

Yuan, Y., He, N., Dong, L., Guo, Q., Zhang, X., Li, B. & Li, L. 2021. Multiscale shellac-based delivery systems: From macro-to nanoscale. ACS nano, 15**,** 18794-18821.

Yüce, E. & Güney, A. 2014. Endüstriyel hammaddelerin zenginleştirilmesi. İçinde: Onal, G., Ateşok, G., Perek, T.(Edt.), Cevher Hazırlama El Kitabı. Yurt Madenciliğini Geliştirme Vakfı, İstanbul**,** 519-578.

Zhang, J., Stevens, M. F. & Bradshaw, T. D. 2012. Temozolomide: mechanisms of action, repair and resistance. Curr Mol Pharmacol, 5**,** 102-14.

Zhang, L., Wang, X.-F., Liu, H., Yu, L., Wang, Y., Simon, G. P. & Qian, J. 2018. Effect of plasticizers on microstructure, compatibility and mechanical property of hydroxypropyl methylcellulose/hydroxypropyl starch blends. International journal of biological macromolecules, 119**,** 141-148.

Zhang, L., Zhou, Y., Shi, G., Sang, X. & Ni, C. 2017. Preparations of hyperbranched polymer nano micelles and the pH/redox controlled drug release behaviors. Materials Science and Engineering: C, 79**,** 116-122.

Power Distribution Company in KARAJ – IRAN : Safety supervisor and risk assessment (2008 – 2012)

CHEGALESH - IRAN : Safety expert and consultant in risk assessment and safety inspector in oil and gas companies (2004 - 2008)

MORATTAB KHODROO - IRAN : Health and Safetey and Environment Supervisor (2002-2004)